Università degli studi di Padova

Dipartimento di Fisica e Astronomia

Tesi di Laurea Magistrale in Fisica

Quorum Sensing communication in bacteria: the role of the system size

Relatore: Prof. Flavio Seno

Correlatore: Dott. Antonio Trovato

Laureando: Mattia Marenda

Anno Accademico 2013/2014

Contents

Introduction

The word communication comes from the latin term *communicare* which means "to share". Philosophically, it assumes different connotations depending on what we are dealing with. If we think about people, the communication concept refers to the speaking or language gestures among individuals; if we think about modern technological devices, everyone knows that it involves signals exchanging through electromagnetic waves, and so on. With all different types of communication, there is a structure given by a sender, a message, a medium and a recipient. In these recent years it was found that also bacteria are able to communicate among them through chemichal signals. It was initially thought they were anomalous systems, since the exchange of chemical signals between organisms was thought as a trait highly characteristic of eucaryotes, but now it is clear that sophisticated communication systems are used by bacteria to coordinate various biological group activities. These systems work through the production and the response of small chemichal molecules and this type of process highly depends on the population's density. To be more precise, when population's density is sufficiently high, signal molecules concentration reaches a threshold value which permits a response by bacteria through the expression of certain specialized genes. The key factor is that under this threshold, genes are not transcribed, therefore their particular effect is visible only over that value of signal concentration. This communication system has been called Quorum Sensing (QS) [16]: it reflects the need of a minimum signal concentration to activate the system [2]. Quorum Sensing expressions are various and in particular they have been shown to be key virulence regulators, in fact QS is an essential mechanism in biofilm formation, antibiotic production, and virulence factor secretion [15]. This means that QS mechanism can represent a target for the development of the agents that treat or prevent bacterial infections, in order to solve the problem when several pathogenic biofilm forming bacteria are often resistant to antibiotics. For this reason, recently, compounds that inhibit Quorum Sensing have received considerable attention as a novel class of antimicrobial agents. Pharmacological inhibition of Quorum Sensing is a particularly attractive approach for the prevention or the treatment of chronic infections with high bacterial cell density, such as cronic lung infections in patients with cystic

fibrosis or chronic wound infections [2].

Therefore, in these years huge developments in the studies of particular biological mechanisms (like QS) have been done. But, what is the role of physics in all this affair? In the recent years physicists have shown interest into the application of physical methods in order to describe complex systems and in particular biological systems. The role of physics in such context is to distinguish between relevant and irrelevant features and to find suitable models in order to describe experimental behaviours. Since one of the most striking aspects of physics is the elegance and the simplicity of its laws, physicists usually start from simple ideas in order to see if these ideas are sufficient to describe even the most complex systems and only later, if necessary, they enrich models with further details. Physicists working in these fields are inspired by Einstein quotation: "Everything should be made as simple as possble, but not simpler." In this thesis, this is what we are going to do with the mechanism of Quorum Sensing commucation.

In particular in this dissertation our aim is to investigate if there could be a system size dependence on QS, beyond the well known cellular density dependence. The idea is to see wether a bigger system with lower density may trigger QS before a smaller system with a higher density does. This fact emerges as a simple consequence of the diffusion laws. In fact if the main ingredient of QS were the diffusion of signal molecules, one would expect size dependent effects. On the basis of this simple idea we proposed some experiments to test our hypothesis, but they turned out to be not in completely agreement with our theoretical expectations. In order to explain these unexpected experimental findings, it is necessary to take in account the full transcriptional network of QS and also the reporting system used to monitor the activation of the bacteria.

This dissertation is organized in the following ways. The first chapter is an introductory discussion in order to explain all the theoretical features necessary to understand our study. In the second one we start from the dynamics of the signal molecules and we explain why system size dependence in QS could be expected as a consequence of molecules diffusion. We also discuss the experiment that we set up, in order to test our theoretical hypothesis and we will show that its results do not fully match our predictions. Then in the third chapter we try to guess if there could be some specific problems in the diffusion model or in the choice of the boundary conditions that might explain the inconsistency of our results. This is not the case, therefore in the fourth chapter we extend the model to introduce the QS trigger mechanism and the subsequent process of gene expression together with the system used to check it. In this way we will see that with these three fundamental steps (signal dynamics, QS trigger, reporting system of gene expression), we are able to find a suitable description for the experimental Quorum Sensing results.

Chapter 1

Biological and Physical features of Quorum Sensing

In this first chapter we deal with the main concepts that will have a central role in this dissertation. The first section explains what Quorum Sensing (QS) is and its role in biology. This section also introduces two particular Quorum Sensing systems and the specific system that we are going to use. The second section presents the concept of diffusion of molecules. This physical effect is to be considered everytime we are working in presence of "colloidal" particles in a fluid. This is the case of the signal molecules of QS for example, or the substrate that we will use as reporting system. In the third section we introduce the concept of molecules degradation and in the fourth one we breifly explain how we can numerically solve diffusion equations.

1.1   Quorum Sensing in bacteria

Recent studies [8] have shown that colonies of the ant *Temnothorax albipennis* are able to emigrate to new nest sites even if active ants organizing the move do not compare all sites. This could seem a very strange behaviour, but it is something very common in nature and this is linked to what we call more generally Quorum Sensing communication. These ants in particular usually live in rock crevices or other cavities which are very fragile and hence it is necessary that ants colonies move frequently to one nest to another. These emigrating colonies can choose the best of several potential nest sites through a collective decision which emerges from a competition between independent groups of ants recruiting nest mates to alternative sites. The question is what rules determine the best site among the different choices. Let's understand the underlying process. Firstly, an active ant which has found a promising site, starts to recruite mates only after

a delay which varies inversely with the site quality. This fact assures in better candidates a stronger positive feedback on population growth. Secondly, a big role is given by the form of recruitment which appears in two different forms: slow tandem runs, in which fellow active ants are carefully led to the new site, and speedier transports, in which the passive majority of the colony is simply taken to the site. At the beginning ants use slow recruitments of active ants by tandem runs, but then, once the group's population has reached the threshold level, they change their recruitment's type and begin a rapid transport of the majority of the colony. In this way the new best nest has been chosen. Ants usually control the groups population (in order to understand when the threshold is rached) through emission and reception of particular pheromones which diffuse through the nest mates or alternatively through antennae's contact. This type of communication is generally referred as Quorum Sensing: a sort of change in behaviour due to the achievement of a particular signal threshold, which in turn is caused by an increase of population.

A similar behaviour can be found in particular strain of bacteria. In this case Quorum Sensing is the regulation of gene expression in response to fluctuation in cell-population density. Quorum Sensing bacteria produce and release chemical signal molecules called autoinducers that increase in concentration as a function of cell density. The detection of a threshold concentration of the autoinducer leads to an alteration in gene expression [1].

This mechanism is therefore characterized by four steps [2]

1. Production of small biochemical signal molecules by the bacteria cell.

2. Release of the signal molecules into the surrounding environment.

3. Recognition of the signal molecules by specific receptors once they exceed a threshold concentration.

4. Changes in gene regulation.

In bacteria, one of the first documented examples of QS was described over 35 years ago. It is the bioluminescence of *Vibrio fischeri* which lives in symbiosis with the Hawaiian Bobtail Squid (see Figure 1.1). These bacteria produce light in the mantle of the squid in order to provide camouflage in the moonlight nights. The squid can match the colour and the brightness of the light from its mantle to the lighting conditions of the night, and hence the squid does not produce a shadow and is safe from predators from below. The enzymes responsible for light production are encoded by a particular luciferase structure operon and light emission was determined to occur only at high cell-population density in response to the accumulation of produced autoinducer signal molecules. Steps were made in
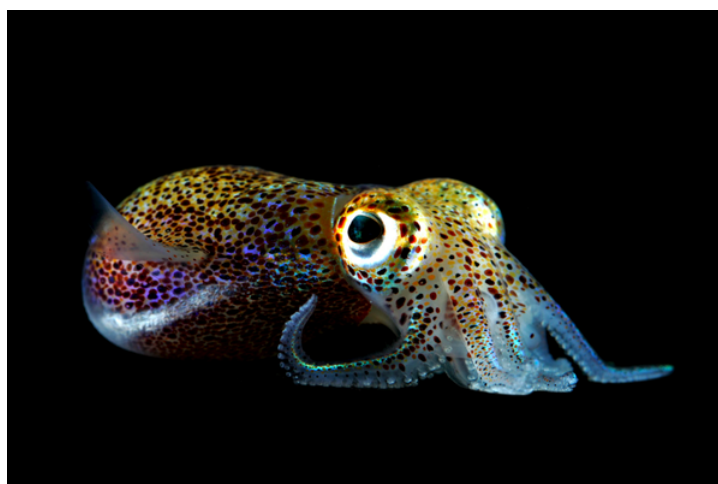
Figure 1.1: Hawaiian Bobtail Squid (*Euprymna scolopes*)

studying this type of communication, finding few other cases of bacteria showing this behaviour for different phenotypes. These systems were considered anomalous, since at that time there was not the belief that bacteria could use cell-cell communications. In fact the exchange of chemical signals between cell/organisms was assumed to be a trait highly characteristic of eucaryotes. The recent explosion of advances has now shown that most bacteria communicate using secreted chemical molecules to coordinate the behaviour of the group. It seems clear that the ability to communicate both within and between species is critical for bacterial survival and interaction in natural habitat. Nowadays we know that a vast assortment of different classes of chemical signals are employed, that individual species of bacteria use more than one chemical signal and more than one type of signal to communicate. Bacteria use QS communication circuits to regulate a diverse array of physiological activities, including symbiosis, virulence, competence, conjugation, antibiotic production, motility, sporulation, and biofilm formation. [1]. For instance, medically much more important species, pathogenic *Staphylococcus aureus* and *Vibrio cholerae*, are capable of forming biofilms controlled by QS. This is a very interesting system, since the control of the QS threshold could be an effective alternative to antibiotic treatment against these pathogenic biofilms.

Nowadays we know that both Gram-positive and Gram-negative bacteria use Quorum Sensing communication circuits. Gram-positive bacteria are a class of bacteria that takes up the crystal violet stain used in the Gram method of bacterial differentiation. This happens because this type of bacteria are characterized by a thick peptidoglycan layer located around their cell membrain. This characteristic let the retaining of the stain, and bacteria assume a violet colour. On the other side, Gram-negative bacteria cannot retain the violet stain after the decolorization step

of the Gram method. What happens is that the alcohol used in the decolorization process degrades the outer membrane of Gram-negative cells, not letting them to retain the violet stain. This occurs because their peptidoglycan layer, located between an inner and an outer membrane, is thinner. In this case identification is due to a counterstain which makes bacteria pink or red. Clearly these two bacterial types exhibits other different characteristics, in particular also in the QS circuit. The main difference is given by the type of the signal molecules (and then also by the circuit). Gram-positive bacteria employ oligopeptides as signals while Gram-negative bacteria use N-acylated homoserine lactones (AHL) [5]. For our interest, in our discussion we will only consider Gram-negative Quorum Sensing circuits.

In the next sections we will first introduce how Gram-negative Quorum Sensing generally works; we will start by decribing the *Vibrio fischeri* Bioluminescence system, since it was the first discovered system and it is considered the model which help to understand all other Gram-negative QS; then we will introduce the *Agrobacterium tumefaciens* QS system and, at the end, we will illustrate the particular QS system that we will use in our dissertation.

1.1.1 Gram-negative bacteria

In the past decade Quorum Sensing circuits have been identified in over 25 species of Gram-negative bacteria with different phenotypes. In every case, except those of *V.harvey* and *M.xantus* the Quorum Sensing circuits identified in Gram-negative bacteria resemble the canonical one of *V.fischeri*. This means that their QS systems contain homologues of two *V.fischeri* regulatory proteins called LuxI and LuxR. The LuxI-like proteins are responsible for the byosinthesis of a specific acylated homoserine lactone signaling molecule (AHL) known as autoinducer. The autoinducer concentration increases with increasing cell-population density. The LuxR-like proteins bind AHL autoinducers when they have achieved a critical threshold concentration, and the LuxR-autoinducer complexes activate target gene transcription. Among the 25 species of bacteria that have a LuxI/LuxR-type circuit the best understood are *Vibrio fischeri*, *Pseudomonas aeruginosa*, *Agrobacterium tumefaciens*, and *Erwinia carotovora*. [1]

An important role is played by signal molecules. All AHL molecules consist in a homoserine lactone part linked to a variable acyl sidechain. Common variations of the N-acyl sidechain structure include chain length and the nature of substituent at the $C-3$ position. These variations determine the biological properties of the AHL within a given population. Several bacteria produce the same AHL signal molecule, although, in each of them it is used to regulate the expression of different biological properties. Other bacteria have shown to produce multiple AHLs, each having different effects on phenotype. [4] Different types of AHL molecules are

listed in Figure 1.2. [5]
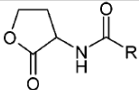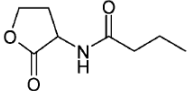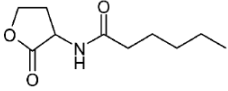
Let's now focus on particular QS systems.

Figure 1.2: Different AHL molecules, main producers and type of circuit

1.1.2 The Vibrio fischeri LuxI/LuxR Bioluminescence System

The first and most intensely studied Quorum Sensing system is that of the bioluminescent marine bacterium *V.fischeri*. This bacterium lives in symbiotic association with a number of eukaryotic hosts, in particular the Hawaiian Bobtail Squid. In each case the host has developed a specialized light organ that is inhabited by a culture of a specific strain of *V.fischeri* at very high cell density. There, the host supplies *V.fischeri* with a nutrient-rich environment where to live and, on the other hand, the role of the bacterium is to provide light to the host. What is important is that light emission is tightly correlated with the population density of the bacteria in the organ, and this phenomenon is controlled by Quorum Sensing. *V.fischeri* bacteria grow in this environment to extremely high cell densities, reaching $10^{11} cell/ml$. When population grows, it produces and release an autoinducer hormone in the extracellular environment. The light organ is the only

place in which the molecule can reach such densities and therefore act as a signal. Accumulation of the autoinducer seems to communicate to the bacteria that they are "inside" the host. Detection of the autoinducer causes a signaling cascade that culminates in the emission of light. Let's see how.
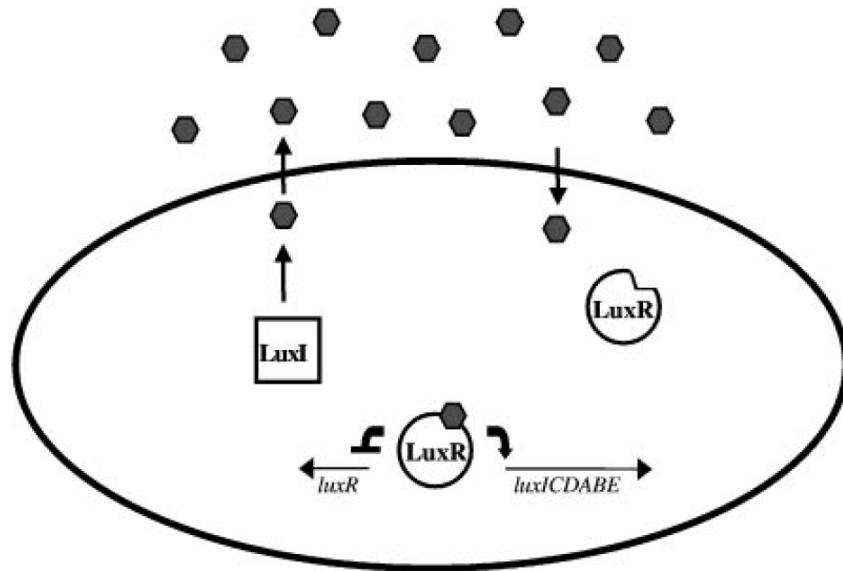
Figure 1.3: Quorum Sensing circuit of *V.fischeri*: the LuxI/LuxR type.

The luciferase enzymes required for light production in *V.fischeri* are encoded by *luxCDABE*, which exists as a part of the *luxICDABE* operon [1]. As we said before, the Quorum Sensing circuit consists in two regolatory proteins called LuxI and LuxR. LuxI is the autoinducer synthase enzyme, and it acts in the production of a particular AHL molecule, the N-(3-oxohexanoyl)-homoserine lactone (OHHL). LuxR functions both to bind the autoinducer and to activate transcription of the *luxICDABE* operon. See Figure 1.3. At low cell densities, the *luxICDABE* is transcribed at a low basal level. Therefore, a low level of autoinducers is produced (via *luxI*), and because the genes enconding luciferase are located directly downstream of the *luxI* gene, only a low level of light is produced. As the bacterium culture increases, autoinducer accumulates to a threshold level $(1 - 10\mu g/ml)$ that is sufficient for detection and binding by the LuxR protein. Interaction of LuxR with the autoinducer reveals the LuxR DNA binding domain, allowing LuxR to

---

[1]An operon is a unit of genomic DNA containing a cluster of genes under the control of a single promoter (the region of DNA that initiates transcription of a particular gene). The genes are transcribed together into a mRNA strand and then translated together in the cytoplasm. The result of this is that the genes contained in a operon are all expressed together.

bind the *luxICDABE* promoter and activate its transcription. This action results in an exponential growth in both autoinducer production and light emission. The LuxR-OHHL complex also acts to negatively regulate expression of *luxR*. This negative feedback loop is a compensatory mechanism in response to the positive feedback. [1]

1.1.3 The Agrobacterium tumefaciens TraI/TraR Virulence System

A.tumefaciens is a plant pathogen that induces crown gall tumors on hosts. The transfer of the oncogene TI plasmid [2] from the bacterium to the host cell nucleus is required for the tumor formation process. Genes on the Ti plasmid let the production of opines in the host plant. These are macromolecules which are consumed as food by the bacteria and are a fondamental part of the QS system. The Ti plasmid also encodes genes that cause the production of hormones that induce host cell proliferation resulting in tumors.

In this type of bacteria, QS controls the conjugal transfer of the Ti plasmid between bacteria. The regulatory proteins TraI and TraR are both located in the Ti plasmid. Conjugation between *A.tumefaciens* cells requires two signals, a host opine and an AHL signal. The AHL signal in this case is N-(3-oxooctanyol)-homoserine lactone (OOHL) and it is the product of the TraI enzyme (the analogous of LuxI) via *traI*. Opines are not necessary only as food source, but also as QS inductor. In fact opines indirectly induce the expression of TraR via specific regulators. We have two Ti plasmids regulated by opines: the octapine-type and the nopaline-type. In the octapine-type Ti plasmid transfer, the opine octapine acts to induce TraR via the activator OccR, where for nopaline-type Ti plasmids, the opine agrocinopine A and B induce TraR expression through the inactivation of the repressor AccR. Hence, Quorum Sensing in *A.tumefaciens* is responsive to both host and bacterial signals, showing that this system works well only in presence of a host.

If we look at the system in a general way, this QS circuit works in the same way of that of *V.fischeri*. In particular, low, basal-level expression of *traI* results in low levels of autoinducers production. After the opine activation of the expression of *traR*, TraR binds to the autoinducer, and the complex induces further expression of *TraI* to make the canonical positive feedback. Target genes regulated by the autoinducer-TraR complex include the *tra* operon, the *trab* operon, and a gene called *traM*. The *tra* operon is necessary for mobilization of the Ti plasmid, while

---

[2]Plasmids are small DNA molecules which are separate from the main chromosomal DNA. They are usually found as small circular, double-strained DNA molecules in bacteria. Their main function is to carry additional information such as genes that may benefit survival of the organism. Morevorer one of their main characteristic is that they can be transmitted from one bacterium to another. This is what happens with the Ti plasmid in *Agrobacterium tumefaciens*.

the *trab* operon encodes the genes necessary for production of the mating pore. TraM acts to downregulate QS by binding to TraR and slowing the binding between TraR and DNA. Therefore we gain an additional level of regulation respect to the LuxI/LuxR circuit. [1]

1.1.4 The Agrobacterium tumefaciens NTL4 β -Gal system

We now describe a system that will be the Quorum Sensing mechanism considered in the following chapters. The choice is simply given by the fact that it is the easiest system to use for experiments. It is also simple to control, since it uses two different bacterial strain, the producer and the reporter. We will describe it focusing only on the main features necessary to understand the mechanism.
In this QS system we consider a mutant strain of *A.tumefaciens* called NTL4, which harbours a recombinant plasmid with a *lacZ:traG* fusion and *traR*. *traG* is a gene which needs the transcriptional activator TraR described above and an AHL for expression. This strain does not produce its own signal molecule, but it can induce the *traG:lacZ* reporter when supplied with an exogenous active AHL. The result is the production of a particular enzyme called β-Galactosidase (β-Gal). This reporter strain responds to different AHL molecules with chain lengths from 4 to 12 carbons. Since this strain lacks in the production of AHL, in the experiments performed for this work a particular bacterial strain of *Rhizobium leguminosarum* was used, which has this characteristic: the *Rhizobium* A34. The fact that the producer and the reporter are two different bacterial strains eliminates the positive feedback which is characteristic of most QS systems. [3]
Apart from the feedback, dynamics is similar to that of all other QS systems of Gram-negative bacteria; once the population is at sufficiently high cell-density, signal concentration reaches the threshold necessary for QS, AHL then binds to TraR, *lacZ:traG* gene is activated and the production of β-Gal enzyme begins.
β-Gal hydrolyzes the β-glycosidic bond formed between a galactose and its organic moiety. Due to this property, it is commonly used in molecular biology as a reporter to monitor gene expression. In particular, to reveal the production of β-Gal enzyme in this QS system and in many other cases, the external substrate X-Gal is usually integrated, since it is an organic compound consisting of galactose linked to a substituted indole. X-Gal is therefore analog to lactose, and can be hydrolized by β-Gal. It then spontaneously dimerizes and is oxidized in presence of oxygen. This product gains a blue colour which is visible by the human eye. Therefore the presence of this blue-coloured product is a proof of the presence of β-Gal. The structure of X-Gal and its complete transformation are shown in Figure 1.4.
As we said before, this QS system is easy to prepare and to control, since it uses producers and reporters separately. Moreover, we need to focus on the fact that the AHL molecules concentration that we are going to deal with, will be around
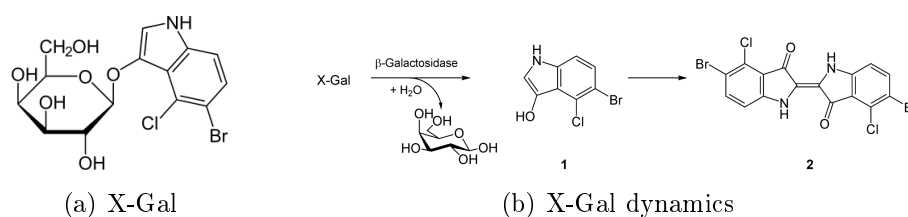
(a) X-Gal   (b) X-Gal dynamics

Figure 1.4: The first figure shows the structure of the X-Gal molecule, while the second one the reaction of hydrolization and dimerization + oxidiation of X-Gal.

nM, which is a very low value. X-Gal technique is therefore a very sensible method able to detect it. On the other hand, it is a very indirect system, since we cannot see the real product of the QS circuit, but the result of its effect on X-Gal. This means that a huge dynamics need to be considered after the QS mechanism.

1.1.5 Quorum Sensing and Physics

Every thing we look, we see a world of amazing complexity. The world contains many examples of complexities at all levels: huge mountain ranges, the delicate ridge on the surface of a sand dune, the salt spray coming off a wave, the interdependencies of financial markets, the true ecologies formed by living things. Each situation is highly organized and distinctive, with biological systems forming a limiting case of exceptional complexity. On the other side, physics main characteristic is the simplicity of its laws. Its aim, since its first developments, has been to find simple and elegant mathematical laws in order to describe natural phenomena in the most general way. Therefore we have that the complexity of the world, in our specific case the biological world, is contrasted with the simplicity of the basic laws of physics. [18]
In these last years physicists have developed an interest into the application of physical methods in describing a lot of complex biological systems. It does not consist in looking for new laws, but in the study of a particular biological phenomenon or structure in order to find a suitable model able to describe its main features. Hence the main difficulty in the application of phyisics to the complex biological world is to find the most important features of the system which let to understand its behaviour: in fact a good theory should provide a way to distinguish between relevant and irrelevant steps and mechanisms, thus advancing our understanding of them. Quorum Sensing communication in bacteria is an example of complex biological phenomenon. In the spirit of what we have just said, our objective will be, if possible, to understand the fundamental behaviour of this communication process starting from simple ideas. At first we will try to study the diffusion of signal molecules in order to see if that will be sufficient to explain

its behaviour.

1.2 The diffusion of molecules

The diffusion of molecules is one of the biggest studies made between the XIX and the XX century. Its importance relies on the fact that it represents the first physical phenomenon which linked the macroscopic world to the microscopic world. On the early XIX century, debates on how the microscopic world should be, were very often among scientists. Some of them believed that matter consisted in small and discrete particles, but others thought about that as an absurd.

Scientists were hoping to find a way to see molecules in order to have a prove of that, but better estimates of the Avogadro's number seemed to demolish the scientific hope. In fact, its value was very huge and as a consequence molecules' volume had to be very small. Even smaller of what they were able to see with microscopes.

In this scenario diffusion was like a miracle, it gave the indirect link that everyone was not expecting anymore. Everything began in 1828 when a botanist named Robert Brown noticed that pollen grains in water were characterized by an erratic and endless movement. Their dimension was around 1 μm in diameter, therefore a microscope was necessary to watch them. However these dimensions were very large compared to atoms. At the beginning, Brown was thinking to see a sort of life process, but some studies helped him to understand his mistake. In fact, the motion of the grain never stopped even if the container was sealed. Moreover, he saw that soot with the same dimension of the pollen grains had the same behaviour. Actually, every particle of the same dimension had the same erratic motion, no matter of what. These types of particles were named generally "colloidal particles". The result was that the theory of life process had to be escluded, but then something else had to be the explanation of this process.

Only around 1860 scientists answered to this question and found the real explanation of the Brownian motion: some of them proposed that this erratic movement was caused by the continuous collisions between the colloidal particle and the molecules of water forced to move by their thermal motion. As a prove of that, there was the fact that experimentally the motion was faster when temperature was higher. However problems and contraddictions were always present. The first involved the dimension of the particles in discussion. Water molecules are very small in respect to the colloidal particle, so it was unbelievable that a collision between the colloidal particle and a molecule of water could macroscopically move the former. The second contraddiction was instead linked to the fact that we are not temporally able to see single collisions. In fact the rate of collisions is around $1/\tau = 10^{12} \ s^{-1}$ due to the small free path of water molecules, given by their small

dimensions. Our eyes can solve only rates smaller than 30 s^{-1}, thus this fact also was unbelievable. These were the two main obsactles in the reception of the theory.

It was necessary the arrival of Albert Einstein in 1905 to explain the missing link and to completely understand these physical phenomena. He understood that the two paradoxes have an elegant and simple solution: they cancel each others. In fact we do no observe every single collision, but we are able to see series of casual collisions; in other words we watch the system at coarse grained time intervals. Therefore what we see are not the single movements, but the rare large displacements which rarely take place in these coarse grained time intervals.

Therefore the conclusion was that effectively diffusion is the manifestation of a random walk, which is originated by the causal collisions with water molecules. It was a huge discover in that period, since it gave a first indirect proof of the molecolar world. Moreover it let the direct calculation of the Avogadro's Number N_A for the first time ever, without any approximation. [19]

We will not discuss the general theory of Brownian Motion, but in the following subsections we will describe why and where diffusion is important when we deal with bacteria and small signal molecules.

1.2.1   Diffusion as gradient of concentration

In our discussion we will work with huge numbers of colloidal particles as signal AHL molecules, the X-Gal substrate and its products. These types of particles are perpetually hit by fluid molecules, causing their diffusion. Therefore, if we neglect interactions among each others, we will have million of random walks indipendent among them. If we suppose their movement led by a gradient of concentration and we impose the conservation of the number of particles, we find the diffusion equation. Let's see why. [19]

It is important to point out that the derivation used here is just an approximation, valid when there are many steps between each observation (in fact that's our case). Imagine, then, that we begin with a three-dimensional distribution that is everywhere uniform in the y, z directions but nonuniform in x. Let's suppose that concentration of particles reduces on the positive x direction and let's subdivide space into imaginary boxes centered at $x - L$, x, $x + L$, . . . The planes labeled a, b represent the (imaginary) boundaries between these boxes (Figure 1.5).

We again simplify the problem by supposing that, on every time step Δt, every particle moves at random for a distance L either to the right or to the left. Thus about half of a given box population hops to the left, and half to the right. And more will hop from the slot centered on $x - L$ to the one centered on x than will hop in the other direction, simply because there are more particles in $x - L$ to begin with.
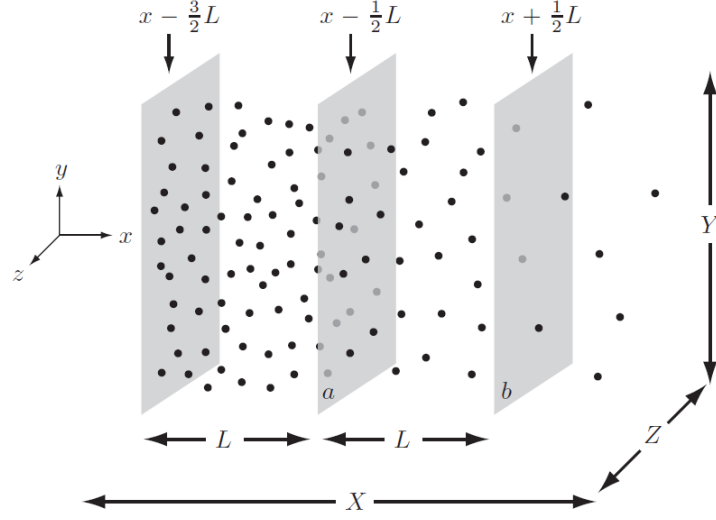
Figure 1.5: Diffusion under gradient of concentration.

1. MOVEMENT UNDER GRADIENT OF CONCENTRATION

Let $N(x)$ be the total number of particles in the slot centered in x, and Y, Z the width of the box in the y, z directions. The net number of particles crossing the box boundary a from left to right is the difference between N evaluated in two nearby points:

$$\frac{1}{2}\left[N(x - L) - N(x)\right]$$

where we count the particles crossing the other way with a minus sign.

We now come to a crucial step: the boxes are totally imaginary, hence we imagine them to be very small ($L \ll 1$). The difference between the $N(x)$ in two nearby points becomes L times the derivative of N :

$$N(x - L) - N(x) \simeq -L\frac{dN(x)}{dx}$$

Since boxes are small, we also suppose that the number of particles inside a box is constant.

Let's now define the density (concentration) of particles, $C(x)$, as the number $N(x)$ in a box, divided by the box volume LYZ:

$$C(x) = \frac{N(x)}{LYZ}$$

Now, the important thing is not really the number of particles crossing the boundary a, but rather the number per unit area of a. The average rate of molecules

crossing a surface per unit area has a special name, the flux, denoted by the letter j. Thus, we can write the flux through the wall a as:

$$j\left(x - \frac{L}{2}\right) = \frac{\frac{1}{2}\left[N(x-L) - N(x)\right]}{YZ\Delta t} = -\frac{1}{2}\frac{L}{YZ\Delta t}\frac{\partial N(x)}{\partial x} = -\frac{L^2}{2\Delta t}\frac{\partial C(x)}{\partial x}$$

If we define the Diffusion Coefficient as $D = \frac{L^2}{2\Delta t}$, we obtain the FIRST FICK'S LAW:

$$j(x) = -D\frac{\partial C(x)}{\partial x} \tag{1.1}$$

where j is clearly the net flux of particles moving from left to right.

If there are more molecules on the left than on the right, then $C(x)$ is decreasing, its derivative is negative, so the right-hand side is positive. That makes sense intuitively: a net drift to the right makes the distribution uniform. If there is a structure in the original distribution, Fick's law says that diffusion will tend to erase it. The diffusion constant D enters the formula, because more-rapidly diffusing particles will erase their order faster.

We assumed that each particle is moving totally independently of the others; we have neglected any possible interactions among the particles, which is appropriate if they are greatly outnumbered in respect to the surrounding solution molecules. Therefore the only thing causing the net flow is simply the fact that if there are more particles in one slot than in the neighboring one, then more will hop out of the slot with the higher initial population. Hops are linked to D and this coefficient is linked to the random forces of the fluid. Hence mere probability seems to be "pushing" the particles.

2. CONSERVATION OF THE NUMBER OF PARTICLES

Looking again at Figure 1.4, we see that the average number $N(x)$ changes in one time step for two reasons: particles can cross the imaginary wall a and they can cross b. Recalling that j refers to the net flux from left to right, we find the net change:

$$\frac{\partial N(x)}{\partial t} = YZ\left[j\left(x - \frac{L}{2}\right) - j\left(x + \frac{L}{2}\right)\right]$$

Once again, we may take the boxes to be small and divide the equation by YZL:

$$\frac{\partial C(x)}{\partial t} = \frac{1}{L}\left[j\left(x - \frac{L}{2}\right) - j\left(x + \frac{L}{2}\right)\right] \simeq -\frac{\partial j(x)}{\partial x}$$

Therefore we get the SECOND FICK'S LAW:

$$\frac{\partial C(x)}{\partial t} = -\frac{\partial j(x)}{\partial x} \tag{1.2}$$

That's the second equation we were seeking.

We can now put the First Fick's Law inside the Second Fick's Law in order to eliminate the flux j.

Therefore, we obtain the DIFFUSION EQUATION:

$$\frac{\partial C(x)}{\partial t} = D\frac{\partial^2 C(x)}{\partial x^2} \tag{1.3}$$

Thus, this is the equation that describes the movements of AHL and of X-Gal (plus its products). Particles are not fixed, but they are involved in an endless casual movement. We will not consider movements of bacteria cells and β-Gal enzyme since they are far bigger than "colloidal" particles. Hence, since we will work in agar environment, we think them as fixed.

1.2.2   Diffusion through a cellular membrane

In chapter 3 we will introduce different models for the diffusing signal molecules of AHL. As we will see, one of the models consists in dividing space between inside and outside bacteria cells. This fact means that we will need a formulation for the movements of the molecules through the cellular membrane. This is what we call diffusion through a cellular membrane.

This type of diffusion is included in an important class of problems in which the concentration remains the same whithin a large region. The diffusing substance enters in one place and exits from another at the same rate. The substance thus diffuses from a source to a sink, with a continuous drop in concentration along the way. There is a steady flux of material through the system, as the flow into each volume element perfectly balances the flow out. Such a system is said to be in a steady state, since the flux is constant and therefore we have the condition:

$$\frac{\partial C(x)}{\partial t} = 0$$

So let's consider a big container with a concentration of particles C_I and a second container with a concentration of particles C_E. They are linked by a very tight channel of length L. See figure 1.6. This is a rude model to describe the inner and the outer part of bacteria cells.

If we are in a situation of steady state we have

$$\frac{\partial^2 C(x)}{\partial x^2} = 0$$

with the boundary conditions of $C(0) = C_I$ and $C(L) = C_E$.

Therefore we obtain a solution of the type:

$$C(x) = Ax + B$$
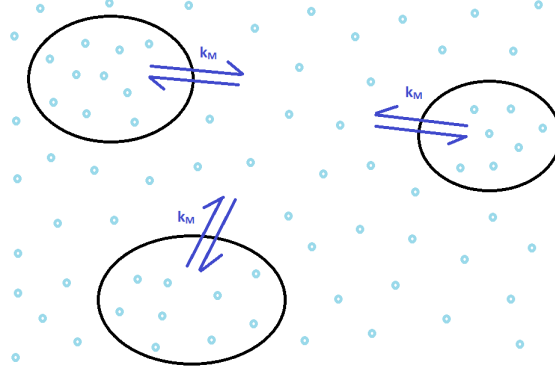
Figure 1.6: Diffusion through cellular membrane.

and if we consider the boundary conditions we arrive to the solution:

$$C(x) = \frac{C_E - C_I}{L} x + C_I$$

Hence we get the constant flux

$$j = -D \frac{\partial C(x)}{\partial x} = -\frac{D}{L} (C_E - C_I)$$

When we talk about membrane channels, it is usually defined the physical quantity

$$P_s = \frac{D}{L} = \text{ Channel Permeability}$$

giving

$$j = -P_s \Delta C = -P_s (C_E - C_I) \tag{1.4}$$

This is the expression of the flux of molecules between the inner and the outer part of a bacteria cell [20]. In our case these molecules will be the AHL signal molecules.

If we suppose that bacteria cells are spheres of radius R_B, we can write the derivate of the number of molecules of AHL inside the cell respect to time t as

$$\frac{\partial N_I}{\partial t} = 4\pi R_B^2 j = -4\pi R_B^2 P_s \Delta C$$

and if we want the time derivate of the inner concentration we need to divide by the volume of the cell V_B:

$$\frac{\partial C_I}{\partial t} = -\frac{4\pi R_B^2}{\frac{4}{3}\pi R_B^3} P_s \Delta C = -\frac{3}{R_B} P_s \Delta C$$

Considering now the fact that we are in a steady state, we get for the time derivate of the number of external molecules

$$\frac{\partial N_E}{\partial t} = -N_B \frac{\partial N_I}{\partial t} = N_B 4\pi R_B^2 P_s \Delta C$$

where N_B is the total number of bacteria that we have in our system.

Again, if we want to obtain the time derivative of the external concentration we need to divide by the total volume of the system V and we get

$$\frac{\partial C_E}{\partial t} = \underbrace{\frac{N_B}{V}}_{\rho_B} V_B 4\pi \frac{R_B^2 P_s}{V_B} \Delta C = \rho_B V_B \underbrace{\frac{3}{R_B} P_s}_{k_M} \Delta C$$

where ρ_B is the density of bacteria and k_M is the rate of transition (it's easy to check that $[k_M] = T^{-1}$).

Thus we obtain the variation in time of the inner and outer concentration caused by the passage of molecules through the cellular membrane:

$$\frac{\partial C_E}{\partial t} = \rho_B V_B k_M \Delta C \tag{1.5}$$

$$\frac{\partial C_I}{\partial t} = -k_M \Delta C \tag{1.6}$$

This equations describe how the concentration changes when the particles are "pushed" by a gradient of concentration, which means diffusion. Since we are moving from inside of bacteria cells to the external environment and viceversa, we notice that the time derivate of C_E is proportional to the density of bacteria and to the volume of the cells. What then lead this movement is the rate k_M (proportional to the diffusion coefficient D) which is hopefully given by the literature.

1.3   Degradation of molecules

In the following chapters we will deal with signal molecules, in particular molecules of the family of the homoserine lactones. Experiments made by the group where I did my thesis work in collaboration with Prof. Andrea Squartini (Department of Department of Agronomy, Food, Natural Resources, Animals and the Environment; University of Padova) showed that these molecules degrade in the time scale that we will consider (hours) [6].

There are several types of degradation, which can be classified in two main categories:

1. The first type is a chemical degradation which can take place both inside

and outside bacteria cells. Molecules can degrade due to chemical reasons with different rates depending on the environment. In this case the simplest way is to think this degradation as proportional to the value of concentration of molecules C, according to the law

$$\frac{\partial C(x,t)}{\partial t} = -kC(x,t) \tag{1.7}$$

where k is the constant rate of degradation and it is measured in s^{-1}. For AHL molecules in agar, its value is known to be $k_e = 1/7 \ days^{-1}$ [6]. While if we consider a degradation of this type inside bacteria cells, this value is unknown.

2. The second type of degradation, suggested by [7] for a problem similar to the one that we consider, is an enzymatic degradation which can take place only inside bacteria cells in our system. In fact bacteria could produce enzymes able to degrade molecules. This behaviour can be treated using the Michaelis-Menten kinetics of enzymatic reactions [20]. Let's see how.
The action of an enzyme E on a substrate S can be thought as a series of chemical reaction of the first order:

$$E + S \underset{k_{-1}}{\overset{k_1}{\rightleftharpoons}} ES \overset{k_2}{\longrightarrow} E + P$$
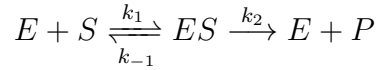
where E represents the free enzyme, S the substrate, ES the bound state enzyme-substrate, P the product after the action of the enzyme on the substrate and k_* are the different reactions rate. We will indicate with $[\cdot]$ the concentration of a given substance.
The velocity of the reaction is given by

$$v = \frac{d[P]}{dt} = k_2[ES]$$

while the variation on time of the concentration of the bound state is:

$$\frac{d[ES]}{dt} = k_1[E][S] - (k_2 + k_{-1})[ES]$$

If we suppose (Aldein hypotheses) that binding is rapid, then $[ES]$ is a steady state for the most part of the time, therefore we got:

$$\frac{d[ES]}{dt} = 0 \ \longrightarrow \ (k_{-1} + k_2)[ES] = k_{-1}[E][S]$$

inverting this formula and introducing the total concentration of enzyme $[E_T] = [E] + [ES]$, we are able to obtain $[ES]$ as a function of the other concentrations:

$$[ES] = \frac{k_1[E_T][S]}{k_{-1} + k_2 + k_1[S]}$$

Hence we can calculate the velocity of the reaction as:

$$v = \frac{k_2[E_T][S]}{\frac{k_{-1}+k_2}{k_1} + [S]}$$

Let's notice that when all the enzyme is in the bound state, we obtain the maximum velocity of the reaction:

$$[ES] = [E_T] \ \longrightarrow \ v_{MAX} = k_2[E_T]$$

Let's then define the MICHAELIS-MENTEN CONSTANT

$$k_M = \frac{k_{-1} + k_2}{k_1}$$

The final result is therefore a velocity of the reaction given by the formula:

$$v = \frac{v_{MAX}[S]}{k_M + [S]}$$

If we suppose that what we call substrate is actually the signal molecule, we obtain the variation on time of the concentration of AHL molecules due to degradation

$$\frac{\partial C(x,t)}{\partial t} = -\frac{v_{MAX}C(x,t)}{k_M + C(x,t)} \tag{1.8}$$

where the minus sign indicates the fact that we are considering the variation of the substrate and not of the product.

This is an alternative way to see degradation inside bacteria. Both parameters in this case are not fixed, as it was k in the previous discussion. Notice the peculiar fact that if we let both parameters going to infinity $v_{MAX}, k_M \to \infty$ in a way that their ratio is constant $v_{MAX}/k_M = k < \infty$, then we obtain again the chemical degradation described in 1. This model for degradation is therefore something more complete even if it is also more complex to study as we can see in chapter 3.

1.4 Numerical solutions for diffusion equations

In Physics we usually encounter several differential equations that are analitically difficult or even impossible to solve. The dream of every physicist is to find a simple and elegant solution to every physical problem of this world, but several times mathematics does not allow this possibility. It is necessary then to find alternatives in order to continue to work even if we are not able to reach our elegant solution. Numerical methods to solve differential equations sometimes are

essentials to understand and solve a physical problem.

The situation is very simple if we deal with first order differential equations in one variable:

$$\frac{dx(t)}{dt} = f(x(t), t)$$

In this case simple methods such as *Euler Method* or *Verlet Method* can be used. And if someone wants a more rigorous and efficient method, he can use the *Runge-Kutta Method*.

Problems and difficulties emerge if we try to solve equations of higher orders and/or with more than one variable. In these cases it is clever to face the equation or the class of equations and to find ad hoc methods suitable for the specific problem.

In the following sections we will find one-dimensional diffusion equations (whose variable C depends on space x and on time t) that we need to solve once given initial conditions and boundary conditions. [22] This features indentify a class of problems which are known as "inital values problems" and they are usually solvable through the scheme in Figure 1.7. From the known spatial values of the variable at $t = 0$, the key is to find an update formula which lets to evolve to successive temporal steps for every position x.
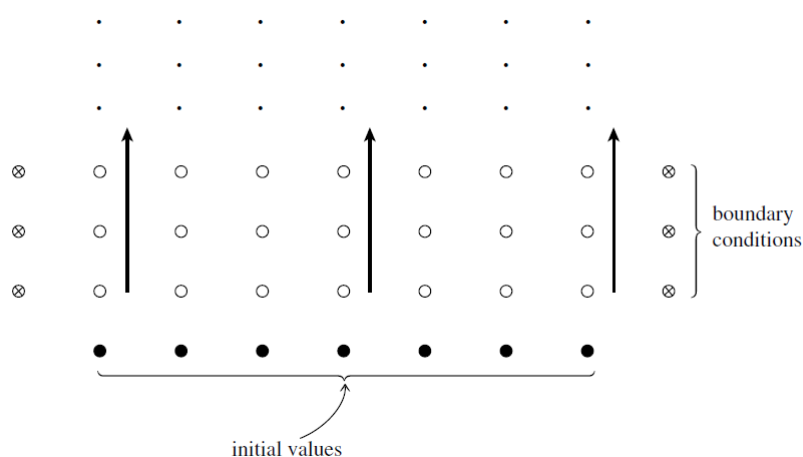

Figure 1.7: Initial value problem (with boundaries).

Let's begin for simplicity with the simplest diffusion equation:

$$\frac{\partial C(x,t)}{\partial t} = D\frac{\partial^2 C(x,t)}{\partial x^2}$$

The easiest way to solve it numerically is to use the *Finite Difference Method* in order to discretize derivatives. Hence if we call j the spatial index in a way that

$x = j\Delta x$ and n the temporal index in a way that $t = n\Delta t$, we get

$$C(x,t) = C(j\Delta x, n\Delta t) = C_j^n$$

We can rewrite in first approximation the temporal derivative as a forward derivative

$$\frac{\partial C(x,t)}{\partial t} \simeq \frac{1}{\Delta t}\left[C(x,t)|_{t+\Delta t} - C(x,t)|_t\right] = \frac{C_j^{n+1} - C_j^n}{\Delta t}$$

While the second spatial derivative can be rewritten as

$$\begin{aligned}
\frac{\partial^2 C(x,t)}{\partial x^2} &\simeq \frac{1}{\Delta x}\left[\frac{\partial C(x,t)}{\partial x}\Big|_{x+\Delta x} - \frac{\partial C(x,t)}{\partial x}\Big|_x\right] = \\
&\simeq \frac{1}{\Delta x}\left[\frac{C(x,t)|_{x+\Delta x} - C(x,t)|_x}{\Delta x} - \frac{C(x,t)|_x - C(x,t)|_{x-\Delta x}}{\Delta x}\right] = \\
&\simeq \frac{C(x,t)|_{x+\Delta x} - 2C(x,t)|_x + C(x,t)|_{x-\Delta x}}{(\Delta x)^2} = \\
&= \frac{C_{j+1}^n - 2C_j^n + C_{j-1}^n}{(\Delta x)^2}
\end{aligned}$$

If we put these last results inside the diffusion equation, we obtain:

$$\frac{C_j^{n+1} - C_j^n}{\Delta t} = D\left[\frac{C_{j+1}^n - 2C_j^n + C_{j-1}^n}{(\Delta x)^2}\right]$$

If we arrange this formula in order to isolate the term at time $n+1$, we obtain the updating formula of the FTCS (Forward Time Centred Space) scheme:

$$C_j^{n+1} = C_j^n + \frac{D\Delta t}{(\Delta x)^2}\left[C_{j+1}^n - 2C_j^n + C_{j-1}^n\right] \tag{1.9}$$

This is an explicit scheme, since it permits to calculate explicitly the value of the concentration at successive times once known the previous one. Figure 1.8 shows the scheme.
Other methods are possible, in fact an alternative to this last scheme is to calculate the spatial derivative at time $n+1$ and not at time n:

$$\frac{C_{j+1}^n - 2C_j^n + C_{j-1}^n}{(\Delta x)^2} \quad \longrightarrow \quad \frac{C_{j+1}^{n+1} - 2C_j^{n+1} + C_{j-1}^{n+1}}{(\Delta x)^2}$$

This change leads to the equation

$$\frac{C_j^{n+1} - C_j^n}{\Delta t} = D\left[\frac{C_{j+1}^{n+1} - 2C_j^{n+1} + C_{j-1}^{n+1}}{(\Delta x)^2}\right]$$
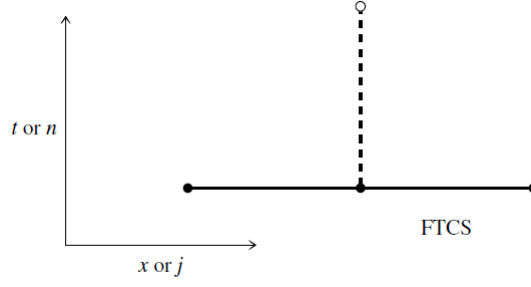
Figure 1.8: FTCS Scheme.

Here the best choice is to isolate the unique n term, in order to obtain the FULLY IMPLICIT scheme (Figure 1.9):

$$C_j^n = C_j^{n+1} - \frac{D\Delta t}{(\Delta x)^2} \left[C_{j+1}^{n+1} - 2C_j^{n+1} + C_{j-1}^{n+1} \right] \qquad (1.10)$$

To solve it, it is convenient to write the system of equations and then to invert
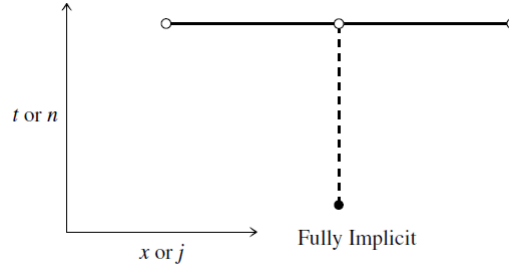
Figure 1.9: FULLY IMPLICIT Scheme.

the matrix which comes out. This calculus is not difficult, because the outcome matrix is tridiagonal.

We usually have boundary conditions in this type of equations, the most common are:

$$\text{REFLECTING BOUNDARY:} \quad \frac{\partial C(x,t)}{\partial x}\Big|_{x=k} = 0$$
$$\text{ABSORBING BOUNDARY:} \quad C(x,t)|_{x=k} = 0$$

and applying the *Finite Difference Method*, they become

$$\text{REFLECTING BOUNDARY:} \quad C_{j(k)}^n = C_{j(k)-1}^n \qquad (1.11)$$
$$\text{ABSORBING BOUNDARY:} \quad C_{j(k)}^n = 0 \qquad (1.12)$$

where we set $j(k)$ the value of j related to k: $k = j(k)\Delta x$.

Initial conditions are easy to describe, since they simply give all the spatial values of C at time $t = 0$, hence $n = 0$. They do not need any type of discretization.

What we have just described is the general theory that teaches us how to solve numerically a diffusion equation. In Appendix A we show how to solve throught FTCS scheme a specific diffusion equation with its boundaries and its initial condition. That equation is also analytically solvable, so we will be able to compare the two results. This could be very interesting, since it shows how two different apporaches, can lead to the same result.

Everything seems clear and easy, but when we try to solve numerically equations with both space and time discretization, we could face some nonsense results. In fact what can emerge is the instability of the scheme due to the fact that errors could amplify instead of reduce. Fortunately, a method which is able to check stablity, exists: the *Von Neumann stability analysis*. This is a procedure used to check the stability of finite difference schemes as applied to linear partial differential equations.[23]

A finite difference scheme is said to be stable if errors do not increase step by step during the calculation. On the other hand if they grow, they are amplified and the calculation becomes unstable. The first useful thing to understand is which numerical errors exist. Actually, there are two types of numerical errors: Discretization error and Round-off error. The first type is the difference between the exact analytical solution of the partial differential equation and the exact (round-off-free) solution of the corresponding difference equation. The second type is the numerical error introduced after a repetitive number of calculation in which the computer is constantly rounding the numbers to some significant figure. For what concerns stability we are clearly interested in the second type.

Let's consider a generic linear partial diffrential equation, which gives rise to a difference equation through a particular scheme. Let's call

$$
\begin{aligned}
C(x,t) = C_j^n &= \text{exact solution of difference equation} \\
N(x,t) = N_j^n &= \text{numerical solution from a real computer with finite accuracy}
\end{aligned}
$$

The round-off error is defined by

$$\epsilon_j^n = N_j^n - C_j^n$$

The idea is that if the error decreases in the temporal step $n \to n+1$, then the scheme is stable; hence we can set the condition of stability as:

$$\left| \frac{\epsilon_j^{n+1}}{\epsilon_j^n} \right| \leq 1$$

Now we need a simple method to see if a scheme is stable or not.

Let's begin noticing that the exact solution C_j^n must satisfy the difference equation, but also N_j^n must satisfy it since the computer is programmed to solve the difference equation. As a consequence of that, the error ϵ_j^n must satisfy the same equation, because we are dealing with linear differential equations. Therefore we get an equation which describes the behaviour of the error ϵ, and this is just the difference equation.

We can think to express the error at a given time and space as a Forier series in the space of moments as follows:

$$\epsilon(x,t) = \sum_m B^t(k_m)e^{ik_m x}$$

and in term of j and n:

$$\epsilon_j^n = \sum_m A^n(k_m)e^{ik_m j \Delta x}$$

where $A(k_m)$ is the amplification factor (which usually is an exponential).

Since the original difference equation is linear and since the round-off error is a solution for the difference equation, then when we substitute the Fourier series in the equation, we got that the behaviour of each term of the series is the same as the series itself. Thus we are allowed to consider just one term of the series and write:

$$\epsilon_j^n = A^n(k)e^{ikj \Delta x} \tag{1.13}$$

In this way the stability condition assumes a very interesting appearance:

$$\left| \frac{\epsilon_j^{n+1}}{\epsilon_j^n} \right| = |A(k)| \leq 1 \tag{1.14}$$

Therefore, the idea of this procedure is the following:

1. We consider the difference equation which comes out from a linear partial differential equation (through a particular scheme).

2. Error ϵ must satisfy the difference equation, therefore we substitute 1.13 in the difference equation.

3. If easily solvable, we need to find $A(k)$ in function of all the other parameters.

4. At the end we have to impose the stability condition 1.14.

Let's try now to applicate the stability analysis to our two schemes.

If we consider the equation for FTCS scheme

$$\frac{\epsilon_j^{n+1} - \epsilon_j^n}{\Delta t} = D \left[\frac{\epsilon_{j+1}^n - 2\epsilon_j^n + \epsilon_{j-1}^n}{(\Delta x)^2} \right]$$

we can put 1.13 in it and then after same calculation we obtain the expression for A:

$$|A| = \left| 1 - 4D\frac{\Delta t}{(\Delta x)^2} sin^2\left(\frac{k\Delta x}{2}\right) \right|$$

which leads to the stability condition

$$\Delta t \leq \frac{1}{2}\frac{(\Delta x)^2}{D} \tag{1.15}$$

It means that we need to pay attention to the amplitude of spatial and temporal intervals. In particular we need to have temporal intervals much smaller than spatial ones. This will be crucial in our study.
If we apply the stability analysis in the case of the FULLY IMPLICIT scheme, it results to be always stable, without any condition. This seems a very interesting fact, but when we try to complicate the diffusion equation, this method is no longer apllicable.

We have just made a brief review on the numerical solutions of diffusion equations. The reason is that we will have to manage very complicated diffusion equations in the following chapters. In particular they will exhibit extra terms which make study harder. One example is the equation:

$$\frac{\partial C(x,t)}{\partial t} = \alpha\rho + D\frac{\partial^2 C(x,t)}{\partial x^2} - kC(x,t)$$

where we have a supplementary constant term and one proportional to C. FULLY IMPLICIT scheme is no longer applicable, so we will have to use the FTCS scheme. Neither *Von Neumann stability analysis* will be usable. But in this latter case, it is useful to remember the result for the simple diffusion equation: we will consider a number of temporal intervals much bigger than that of spatial intervals in order to reach the stability. This is not a rule, but it works anyway. Beyond these difficulties, FTCS scheme is easy to apply and lets to find the numerical solution, even with more complicated equations, and the "empiric" rule is useful to find stability.

Chapter 2

The system size dependence of Quorum Sensing

The previous chapter was an introduction to the main concepts we are going to deal with. They were strictly necessary to understand what follows.

Now we will focus on the possible system size dependence of Quorum Sensing, which means that the dimension of the system could directly affect Quorum Sensing mechanism. The first question is why we should expect this behaviour. We start from a simple idea: we suppose that diffusion of signal molecules is the only fundamental property which has to be taken in account to describe the mechanism. This fact automatically implies a size dependence of QS. In this chapter we will show the reason of this last statement, using two simple theoretical models. After that, we discuss the experiment we proposed to verify if there is such a size dependence.

2.1 The theoretical framework of system size dependence

We start from the strong hypotheses that QS is mainly ruled by the diffusion of AHL and that the biological network which follows the reaching of quorum threshold is relatively less important. In this way we can prove, as a merely consequence, that the size of the bacterial colony has a fundamental role in the QS mechanism. We can see it in two different ways. The first one is a generic 3-dimensional model which can be mapped on a simple electrostatic system while the second one is a 1-dimensional model similar to the experimental device that we set up. Clearly, if our experiment proved size dependence, we would confirmed the primary importance of signal molecules diffusion.

2.1.1 The 3-dimensional diffusing system of AHL

Let's consider a bacterium which is able to produce AHL molecules and which is fixed in the origin of a 3-dimensional reference system (x, y, z). We suppose that the bacterium size is so small that we are allowed to consider it as a point. If we consider that the production rate α of AHL is constant, the equation of diffusion of signal molecules assumes the form:

$$\frac{\partial C(x, y, z, t)}{\partial t} = D\nabla^2 C(x, y, z, t) + \alpha\delta(\vec{r})$$

where C is the concentration of signal molecules, D is the diffusion coefficient and $\delta(\vec{r})$ is the Dirac-delta. The initial condition is $C(x, y, z, 0) = 0 \; \forall \; x, y, z$
We need to solve an equation of the form:

$$\frac{\partial C(x, y, z, t)}{\partial t} = D\nabla^2 C(x, y, z, t) + g(x, y, z)$$

Under the hypotheses that the initial concentration is null everywhere and that g does not depend on time, its solution is [21]

$$C(x, y, z, t) = \frac{1}{4\pi D} \int_{\mathbb{R}^3} \frac{g(\eta, \xi, \varsigma)}{r'} \left[1 - \Phi\left(\frac{r'}{2\sqrt{Dt}}\right) \right] d\eta d\xi d\varsigma$$

where we used the Error Function

$$\Phi(\alpha) = \frac{2}{\sqrt{\pi}} \int_0^\alpha e^{-p^2} dp$$

and we set for simplicity of notation

$$r' = \sqrt{(x - \xi)^2 + (y - \eta)^2 + (z - \varsigma)^2}$$

In our situation we have that

$$g(x, y, z) = \alpha\delta(\vec{r})$$

Therefore if we subsitute the expression of g, due to Dirac-delta properties we obtain

$$C(r, t) = \frac{\alpha}{4\pi Dr} \left[1 - \Phi\left(\frac{r}{2\sqrt{Dt}}\right) \right] \tag{2.1}$$

This equation describes the concentration of AHL in function of time t and of distance r from the source. It clearly has a spherical simmetry.
If we let time to go to infinity, we obtain signal concentration at equilibrium

$$C(r, t = \infty) = \frac{\alpha}{4\pi Dr} \tag{2.2}$$

Since diffusion equation is linear, if one has many sources (N, for example), in order to obtain signal concentration in a given point r and a given time t, one needs to sum the contribution of all sources:

$$C(\vec{r}, t) = \sum_{i=1}^{N} C(\vec{r_i}, t)$$

where $\vec{r_i}$ is the position of the i-th source in respect to $\vec{r}$.

Thinking again that bacteria are very small and fixed in their position, we can represent them with a uniform distribution of density ρ, which we suppose to be a sphere of radius R. It is not difficult to obtain the concentration in function of the distance from the centre of the sphere. To make this calculus we should let the sum written above to become continous:

$$C(\vec{r}, t) = \rho \int C(r - r', t) dV$$

which means to calculate in the limit of very large t the equation

$$C(r, t) = \frac{\rho \alpha}{4 \pi D} \int_0^R \int_0^\pi \int_0^{2\pi} \frac{1}{|\vec{r} - \vec{r'}|} \left[1 - \Phi \left(\frac{|\vec{r} - \vec{r'}|}{2\sqrt{Dt}} \right) \right] r'^2 dr' sin\theta d\theta d\phi \quad (2.3)$$

where $\vec{r'}$ is the distance of a source from the centre of the sphere.

This sum can be avoided noticing the analogy with an electrostatic system. As we can see from equation 2.2, each bacterium is giving a contribution of type $1/r$; therefore this issue is formally the same of an electrostatic problem where there is a uniform spherical distribution of charge Q. In fact every charge generates a potential of the form

$$\Psi(r) = \frac{q}{4 \pi \varepsilon_0 r}$$

Computing the concentration of AHL molecules generated by a spherical colony of bacteria in function of r corresponds to compute the electrostatic potential generated by a uniformly charged sphere. Applying the Gauss Theorem, we get that the electrostatic field generated by a uniformly charged sphere of radius R inside and outside the sphere is

$$\vec{E}(r) = \begin{cases} \frac{Q}{4\pi\varepsilon_0} \frac{1}{r^2} \vec{e_r} & \text{if } r > R \\ \frac{Q}{4\pi\varepsilon_0} \frac{r}{R^3} \vec{e_r} & \text{if } r \leqslant R \end{cases}$$

Therefore if we compute the electrostatic potential supposing "open boundary conditions" (in other words that its value is 0 at $r = \infty$)

$$\Psi(r) = - \int_\infty^r \vec{E}(s) d\vec{s}$$

we then get

$$\Psi(r) = \frac{\rho}{6\varepsilon_0}(3R^2 - r^2)$$

where $\rho = \frac{3Q}{4\pi R^3}$

On the other hand, if we suppose "absorbing boundary conditions" (which means that potential is 0 when we are on the surface of the sphere) we just need to remove from the previous result the value of the potential in R. Hence

$$\begin{aligned}
\Psi(r) &= \frac{\rho}{6\varepsilon_0}\left(3R^2 - r^2\right) - \Psi(R) = \\
&= \frac{\rho}{6\varepsilon_0}\left(3R^2 - r^2\right) - \frac{\rho R^2}{3\varepsilon_0} = \\
&= \frac{\rho}{6\varepsilon_0}\left(R^2 - r^2\right)
\end{aligned}$$

The analogy leads for our system to the result in case of "open boundary conditions"

$$C(r) = \frac{\alpha\rho}{6D}(3R^2 - r^2) \tag{2.4}$$

and in case of "absorbing boundary conditions"

$$C(r) = \frac{\alpha\rho}{6D}(R^2 - r^2) \tag{2.5}$$

Equations 2.4 and 2.5 mean that for a given density of bacteria AHL concentration in a specific point (e.g. in the centre of the sphere) is higher for larger spheres. Thus a larger sphere with lower density may trigger Quorum Sensing before a smaller sphere with higher density.

2.1.2 The 1-dimensional lane with boundaries

Let's now consider the 1-dimensional system which will lead us to the analogous result of the previous section. We also study this system, because it will be the one that we reproduce in our experiment.

So let's consider a 1-dimensional lane on the x axis of length h with an absorbing boundary in $x = 0$ and a reflecting boundary in $x = h$. See figure 2.1.

Let's suppose to have a uniform colony of bacteria inside the lane and that they are able to produce AHL molecules with a constant rate α. Let's also introduce the fact that signal molecules chemically degrade, therefore with a constant rate k and proportionally to molecules concentration. Again we do not consider the entire mechanism, but we only focus on the diffusing mechanism of signal molecules. In this case we obtain a generic diffusion equation for AHL molecules that is

$$\frac{\partial C(x,t)}{\partial t} = \alpha\rho + D\frac{\partial^2 C(x,t)}{\partial x^2} - kC(x,t) \tag{2.6}$$
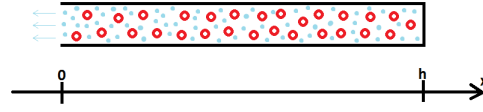
Figure 2.1: A simple draw of the 1-dimensional lane with an absorbing boundary and a reflecting one. Red circles represent fixed bacteria, while blue dots represent diffusing signal molecules.

with boundary conditions

$$\begin{cases} C(x,t)|_{x=0} = 0 & \text{Absorbing condition} \\ \frac{\partial C(x,t)}{\partial x}|_{x=h} = 0 & \text{Reflecting condition} \end{cases}$$

and initial condition

$$C(x,0) = 0 \ \forall x$$

This equation means that the concentration of signal molecules is influenced in time and in position by three different factors: the constant production of molecules, their spatial diffusion end their degradation.

This equation is easily solvable at time equilibrium, in fact if we set the condition

$$\frac{\partial C(x,t)}{\partial t} = 0$$

we get the ordinary second order differential equation

$$\frac{\partial^2 C(x,t)}{\partial x^2} - \frac{k}{D} C(x,t) + \frac{\alpha \rho}{D} = 0$$

with solution

$$C(x) = C_0 \left[1 - \frac{cosh[\lambda(h-x)]}{cosh(\lambda h)} \right]$$

where $C_0 = \frac{\alpha \rho}{k}$ and $\lambda = \sqrt{\frac{k}{D}}$

In figure 2.2 we can see its behaviour for a given length h of the lane and a adequate [1] choice of parameters k and α. Supposing that the fluid inside the lane (experimentally thought as a cylinder) is a mixture of agar and water, the value of the diffusion coefficient of AHL molecules is supposed to be given by [6] and is $D = 1,08 \ mm^2/s$.

However, if we think to observe cylinders where concentration of molecules is

---

[1]adequate parameters means that these are those parameters that we found to be suitable for the descriptions of experimental data (a posteriori choice)
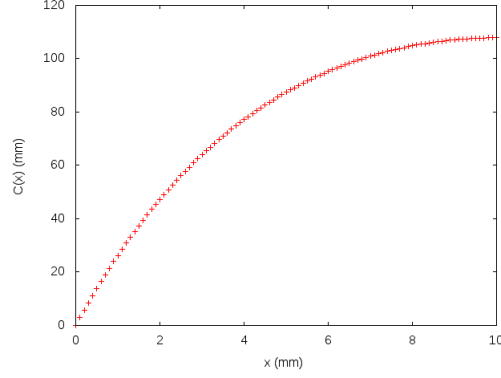
Figure 2.2: Concentration of signal molecules in a lane with $h = 10 \; mm$. Parameters: $\rho = 10^8 \; cell/l$, $k = 0,05 \; h^{-1}$ and $\alpha = 7 \cdot 10^{-9} \; nMol/(cell \cdot h)$

higher, therefore at the reflecting boundary $x = h$, we can obtain concentration in function of the length h of the lane:

$$C(h) = C_0 \left[1 - \frac{1}{cosh(\lambda h)} \right]$$

If we suppose to have $\lambda h \ll 1$, therefore considering for example very short lanes, we can then expand the term

$$\frac{1}{cosh(\lambda h)} = sech(\lambda h) = 1 - \frac{1}{2}(\lambda h)^2 + \frac{5}{24}(\lambda h)^4 - \frac{61}{720}(\lambda h)^6 + \ldots \simeq 1 - \frac{(\lambda h)^2}{2}$$

obtaining the result

$$C(h) \simeq \frac{\alpha}{D} \rho h^2 \tag{2.7}$$

Again, we find out not only a dependence on the density of bacteria cells but also on the length of the lanes, therefore on the size of the system. In figure 2.3 the dependence of AHL concentration on h and the parabolic behaviour for small length for a suitable choice of parametres are shown.

In case of non-temporal equilibrium equation 2.6 is not easily analitically solvable, however a numerical solution can be found. The out of equilibrium solution $C(x,t)$ can be numerically calculated using the FTCS scheme shown in section 1.4. We obtain the update formula

$$C[i][j+1] = C[i][j] + \alpha \rho \Delta t + \frac{D \Delta t}{\Delta x^2}(C[i+1][j] - 2C[i][j] + C[i-1][j]) - k \Delta t C[i][j]$$

where i is the spatial index which goes from 0 to P; it indicates a space $x = ih/P = i\Delta x$ which in turn goes from 0 to h with jumps of Δx. On the other side j is the
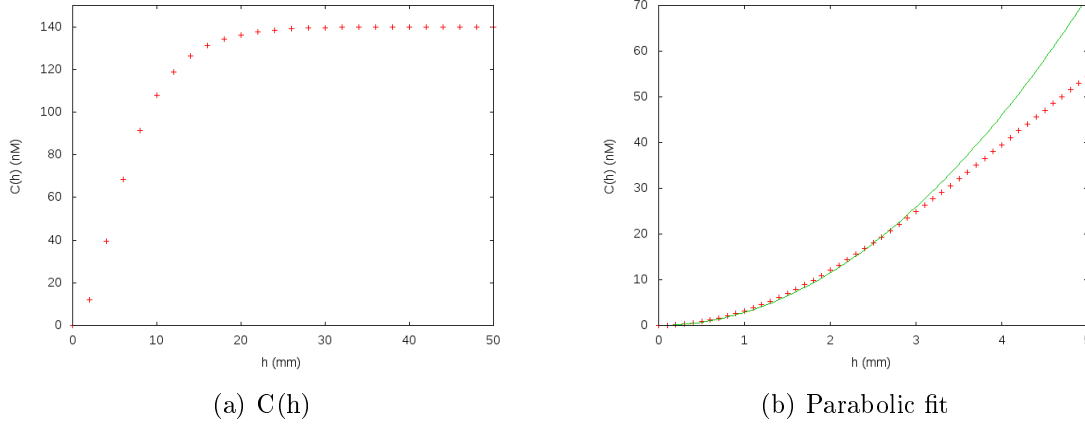
(a) C(h)

(b) Parabolic fit

Figure 2.3: Figure a) shows the value of C in function of h for $h \in [0, 50]$. Figure b) shows the parabolic fit $f(h) = (2,87 \pm 0,02)h^2$ on red data. Fit is made using values between 0 and 3. Parameters: $\rho = 10^8$ $cell/l$, $k = 0,05$ h^{-1} and $\alpha = 7 \cdot 10^{-9}$ $nMol/(cell \cdot h)$.

temporal index which goes from 0 to M; it indicates a time $t = jt_{MAX}/M = j\Delta t$. It takes values from 0 to t_{MAX} with jumps of Δt. This permits to calculate the out of equilibrium concentration, once given initial conditions

$$C[i][0] = 0 \ \forall i \in [0, P]$$

and boundary conditions

$$\begin{cases} C[0][j] = 0 & \forall j \in [0, M] \text{ Absorbing condition} \\ C[P][j] = C[P-1][j] & \forall j \in [0, M] \text{ Reflecting condition} \end{cases}$$

If we are interested in $C(h, t)$, we just need to consider $C[P][j]$ for a given length h.

In Figure 2.4 (temporal) equilibrium and out of equilibrium solutions $C(h, t)$ are shown. We can see that a parabolic behaviour remains out of equilibrium, too. The difference between the two situations is that out of equilibrium saturation comes earlier and at a lower value.

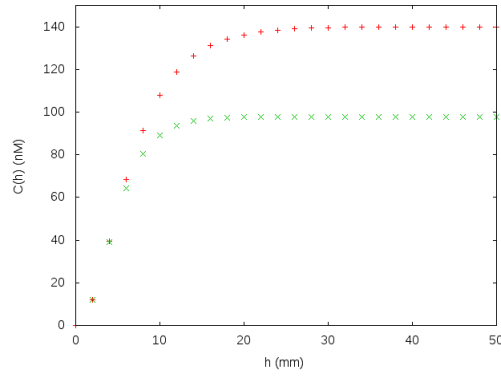This study is therefore a second proof of the possible size depence of Quorum Sensing.

Figure 2.4: Red dots represent equilibrium behaviour, while green dots represent $C(h)$ behaviour for $t = 24h$. Parameters: $\rho = 10^8\ cell/l$, $k = 0,05\ h^{-1}$ and $\alpha = 7 \cdot 10^{-9}\ nMol/(cell \cdot h)$.

2.2 The experimental evidence of system size dependence

Results of the previous section lead to think seriously about the size dependence of Quorum Sensing. If our results were experimentally validated, we could state that diffusional signal dynamics is the main ingredient in modelling QS. Therefore, to verify this possibility, what we tried to do was to build the 1-dimensional lane with a reflecting boundary and an absorbing one to see if size dependence would have come out. This experiment was set up by Prof. Andrea Squartini and his group (Department of Agronomy, Food, Natural Resources, Animals and the Environment; University of Padova).

As we can see in Figure 2.5, the idea was to build a big beaker containing $500ml$ of agarose dissolved in water at a final concentration of $0,7\%$. On the surface of this substance a series of ployethylene cylinders with diameter $9mm$ were fixed. These cylinders are the lanes of the 1-dimensional model discussed above. A different height of the material inside cylinders means a different system dimension. They are clearly not one dimensional systems, but we are allowed to think as they were, beacause their lateral side can be considered as a totally reflecting surface. The Quorum Sensing mechanism takes place inside these cylinders and it is of the type discussed in Section 1.1.4, therefore a β-Gal circuit. It is necessary to precise that the role of the big beaker is to create the condition of absorbing boundary: the cylinders' base in contact with baker's agar is the absorbing boundary, while the base in contact with air is the reflecting one. The first statement is based on the fact that the volume of the baker is sufficiently large to suppose it as an infinite reservoir. The second one is proved by previous experimental results made by the
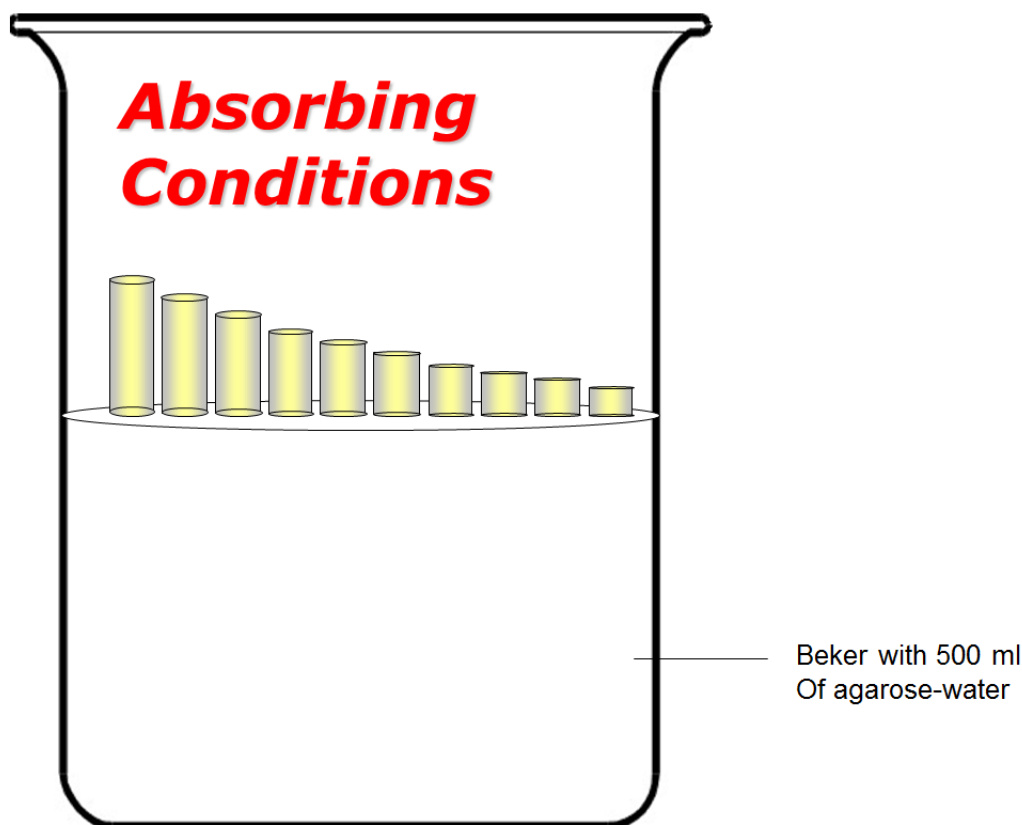
Figure 2.5: Baker with cylinders

group who I worked with [6]

The producer bacterial strain for this experiment is *Rhizobium leguminosarum* A34, since it is able to produce OOHL signal molecules. Reporter bacteria were different from producers, we used *Agrobacterium tumefaciens NTL4*, the mutant which is able to respond to OOHL and activate the production of β -Gal under the Quorum Sensing mechanism. To reveal the enzyme production, X-Gal substrate is necessary, too. *R.leguminosarum* A34 and *A.tumefaciens* NTL4 were taken from stocks stored at the temperature of $-80°C$, incoulated in sterilised TY medium [2] and AB medium [3], respectively, and grown overnight with shaking at $30°C$. The following day $10ml$ of grown *R.leguminosarum* A34 were centrifuged for $15min$ at $5000rpm$ in order to remove the TY medium and $10ml$ of physiological solution were added. Afterwards, bacteria concentration was calculated

---

[2]pH 6,8: $5g/l$ Tryptone $+ 3g/l$ Yeast Extract $+ 0,7g/l\ CaCl_2 + 0,9g/l\ 2H_2O$

[3]$3g/l\ K_2HPO_4$, $1g/l\ NaH_2PO_4$, $1g/l\ NH_4Cl$, $0,3g/l\ MgSO_4 - 7H_2O$, $0,15g/l\ KCl$, $0,01g/l\ CaCl_2$, $2,5mg/l\ FeSO_4 - 7H_2O$, $0,5\%\ Glucose$

through the Thoma Chamber with the help of an optical microscope [4]. Proceeding through diluition, three tubes with different producers concentrations were created: $10^7 cell/l$, $10^8 cell/l$ and $10^9 cell/l$.
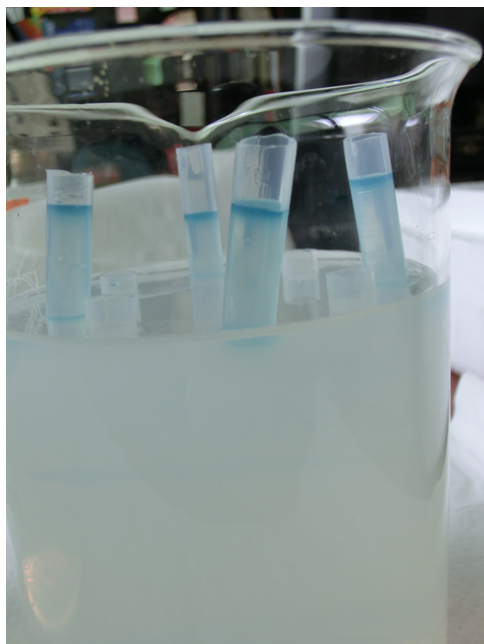
(a) $10^8 cell/l$ (b) $10^7 cell/l$

Figure 2.6: The two figures show at $t = 92h$ the experimental results for two different concentrations of producers: $10^8 cell/l$ and $10^7 cell/l$

In a flask, $6, 55ml$ of AB medium $+ 0, 7\%$ agarose were added with $3, 35ml$ of grown *A.tumefaciens* NTL4, $100\mu l$ of *R.leguminosarum* A34 with the desired concentration, $30\mu l$ of $20mg/ml$ X-Gal (final concentration $60\mu g/ml$). Quantities were set up in order to have a concentration of reporters of $10^{11} cell/l$. Two other flasks were used to obtain other concentrations of producers. In this way we obtained three flasks which differed for the density of producers.
Every mixture was then pippeted with appropriate calculations inside cylinders in order to obtain 10 different heights, from $2mm$ to $20mm$ every $2mm$. Therefore, at the end, we obtained three different bakers, each one containing ten cylinders, which in turn had inside QS systems of different heights. Each beaker differed from the others for the density of producers inside its cylinders.
After the setting up of the experiment, the Quorum Sensing mechanism and the successive action of β-Gal on X-Gal showed a blue-coloured product after several

---

[4] $100\mu l$ bacteria $+ 800\mu l$ phys. sol. $+ 100\mu l$ Ethanol $+ 10\mu l$ Methylene blue

Height (cm)		$\rho_p = 10^7$ cell/l			$\rho_p = 10^8$ cell/l			$\rho_p = 10^9$ cell/l	
		t = 24 h	t = 92 h		t = 24 h	t = 92 h		t = 24 h	t = 92 h
0,2									SLIGHTLY ON
0,4					SLIGHTLY ON	SLIGHTLY ON		SLIGHTLY ON	SLIGHTLY ON
0,6			SLIGHTLY ON		ON	ON		STRONGLY ON	STRONGLY ON
0,8			ON		ON	ON		STRONGLY ON	STRONGLY ON
1,0			STRONGLY ON		ON	ON		STRONGLY ON	STRONGLY ON
1,2			STRONGLY ON		ON	ON		STRONGLY ON	STRONGLY ON
1,4			STRONGLY ON		ON	ON		STRONGLY ON	STRONGLY ON
1,6			STRONGLY ON		ON	ON		STRONGLY ON	STRONGLY ON
1,8			STRONGLY ON		ON	ON		STRONGLY ON	STRONGLY ON
2,0			STRONGLY ON		ON	ON		STRONGLY ON	STRONGLY ON

OFF

SLIGHTLY ON

ON

STRONGLY ON

Figure 2.7: Experimental results

hours. The blue-coloured substance appeared at first on the top of the cylinders and then diffused through their entire length. The time of "turning on" depended on the density of producers and on the different heights of the mixture inside every cylinder. Figure 2.6 shows the experimental behaviour for two different beakers at the same time. Density of producers is ten times higher in the first beaker than in the second one.

Focusing on the appearance of the colour at the top of cylinders and thinking about dividing the "turning on" in different scales, we can resume the experimental results in tables as shown in Figure 2.7. The table is divided by producers' density and by observation time ($24h$ and $92h$). Each row represents a different length of the system. The size dependence appears in a very evident way. For example, at $92h$ the system $1,0cm$ high with $\rho_p = 10^7 cell/l$ is *strongly on* while the system $0,4cm$ high with $\rho_p = 10^8 cell/l$ is just *slightly on*. This fact should prove that size has an important role on QS. However this is not exactly the desired behaviour, because the size dependence seems to be too strong. When system height is small, twe should obtain the behaviour of equation 2.7:

$$C(h) \simeq \frac{\alpha}{D}\rho h^2$$

However experimental results, as we see from the observation made above, seem to have a stronger dependence on height. In fact a square dependence should imply that if for $\rho = 10^8$ cell/l QS turns on at $h = 6$ mm, then for $\rho = 10^7$ cell/l phenomena should start in much longer cylinders than what observed. This fact is essential since it opens a problem to understand what this mechanism exactly is.

First of all it is necessary to improve the model of AHL diffusion with the aim of finding a stronger dependence on the lane's length. This will be the main topic of the next chapter. After that, the study must be completed considering the entire circuit. Hence, in chapter 4 we will discuss what follows QS, therefore the $\beta - Gal$ production and its action on X-Gal. Diffusion of X-Gal and its products will be crucial to explain experimental results.

Chapter 3

Models for signal molecules dynamics

In the previous chapter we saw that diffusion of signal molecules implies a system size dependence of Quorum Sensing. Our experiment seems to point a size dependence, even if its results are not in full agreement with our predictions.

In this chapter we try to improve the model introduced in section 2.1.2 in order to find a better description of the experimental behaviour. The main goal is to try to reproduce better results at small lengths, since there we completely missed to fit experimental data. In the following sections we exhibit different models which use the first one as basis (we will refer to it as Model 0). The first aspect we can think about is to divide the space in two or three different environments and to modify the type of degradation. The second one is to to eliminate the concept of absorbing boundary and fix a flux of particles on that boundary. These ideas generate two different models which show different approaches to the problem. As we will see, none is perfect to describe the experiment by its own, but acceptable results are reached. The introduction of the dynamics after Quorum Sensing will be the key of the problem, as we will see in the last chapter.

3.1   The Inside-Outside Model

The first idea is to build a model dividing space in two or three different environments. To be more precise, it is reasonable to think that laws which govern the behaviour of molecules, could be different inside and outside bacteria cells and their difference might be relevant for the overall process. For example, if AHL molecules degraded only inside cells, we should explicitly consider these facts, since we would have a degradation dependent on bacteria density.

3.1.1 Producers and external environment

Let's consider at the beginning just the space inside producers and the exterior. We suppose to have a production of AHL molecules with a constant rate α and a chemical degradation [1] with a constant rate k. Both these mechanism are supposed to take place inside producers. In this case we obtain a system of differential equations: the first equation concerns the variation on time of AHL concentration inside bacteria $C_p(x,t)$ while the second one the variation on time of AHL concentration in the external environment $C_e(x,t)$. We suppose that this latter is the quantity which trigger the Quorum Sensing mechanism. The two equations are:

$$\begin{cases} \frac{\partial C_e}{\partial t} = D\frac{\partial^2 C_e}{\partial x^2} - k_M(C_e - C_p)\rho_p V_B \\ \frac{\partial C_p}{\partial t} = \frac{\alpha}{V_B} - k_M(C_p - C_e) - kC_p \end{cases} \qquad (3.1)$$

with boundary conditions

$$\begin{cases} C_e(x,t)|_{x=0} = 0 & \text{Absorbing condition} \\ \frac{\partial C_e(x,t)}{\partial x}|_{x=h} = 0 & \text{Reflecting condition} \end{cases}$$

and initial condition

$$C_e(x,0) = C_p(x,0) = 0 \; \forall x$$

where ρ_p is the density of producers and V_B the single bacteria volume. In the equations we included a diffusion, a production, a degradation term and the two terms wich describe diffusion through a cellular membrane (see equations 1.6). The value of the passage rate k_M (for AHL) is given by [6] and it is $k_M = (20\ s)^{-1} = 180\ h^{-1}$. We need to stress that we think bacteria as very small entities, therefore we do not consider diffusion inside bacteria cells. $C_p(x,t)$ simply represents AHL concentration inside a bacteria cell in position x.

This system can be solved numerically, but we can manage it analitically if we introduce the approximation (validated below) of internal equilibrium. Therefore, we put

$$\frac{\partial C_p}{\partial t} = 0$$

Figure 3.1, obtained by numerically solving system 3.1, shows for an adequate [2] choice of α and k that temporal equilibrium of C_p is effectively reached in a very short time. This result is clearly obtained by numerical solution of the coupled differential equations. Therefore in the steady-state case we have

$$\frac{\alpha}{V_B} - k_M(C_p - C_e) - kC_p = 0$$

---

[1]Later on we will also introduce a more realistic enzymatic degradation.

[2]adequate parameters means that these are those parameters that we found to be suitable for the descriptions of experimental data (a posteriori choice)
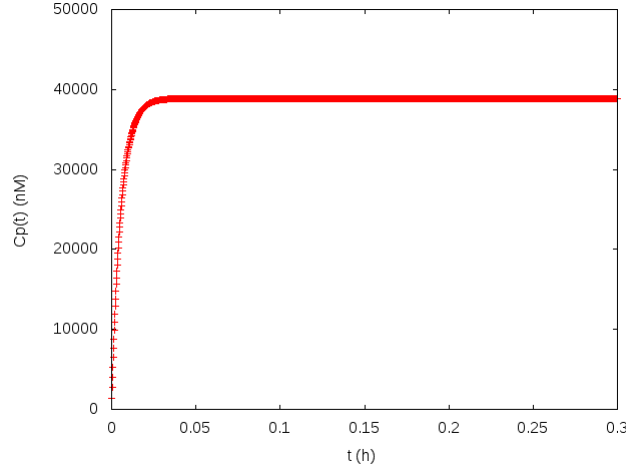
Figure 3.1: Concentration of AHL molecules inside bacteria for a lane $h = 10\ mm$ in position $x = 5\ mm$. Parameters are $\rho_p = 10^8 cell/l$, $\alpha = 7 \cdot 10^{-9} nMol/(cell \cdot h)$, $k = 0,05\ h^{-1}$. Equilibrium is fully reached in a time less shorter than 1 hour. In our study we are interested in times longer than hour.

In particular we want to find C_p in function of C_e:

$$C_p = \frac{\alpha + V_B k_M}{V_B(k + k_M)} C_e$$

We can then put this relation inside equation 3.1 in order to obtain the partial differential equation:

$$\frac{\partial C_e}{\partial t} = \underbrace{\frac{\alpha k_M}{k + k_M}}_{\tilde{\alpha}} \rho_p + D\frac{\partial^2 C_e}{\partial x^2} - \underbrace{\frac{k_M k}{k + k_M} \rho_p V_B}_{\tilde{k}} C_e \qquad (3.2)$$

Hence we obtain an equation similar to that of Model 0:

$$\frac{\partial C_e}{\partial t} = \tilde{\alpha}\rho_p + D\frac{\partial^2 C_e}{\partial x^2} - \tilde{k}C_e$$

but now we have an effective rate of production $\tilde{\alpha}$ and an effective degradation rate $\tilde{k}$. The first one is proportional to the real production rate through a coefficient which depends on k_M and k. The second effective rate is again proportional to the old one by the same coefficient as $\tilde{\alpha}$, but it is also proportional to the bacterial density and volume. This last fact is the real improvement of this model, since Andrea Squartini and his group [9] found out that degradation of AHL molecules depends on the density of Quorum Sensing bacteria.
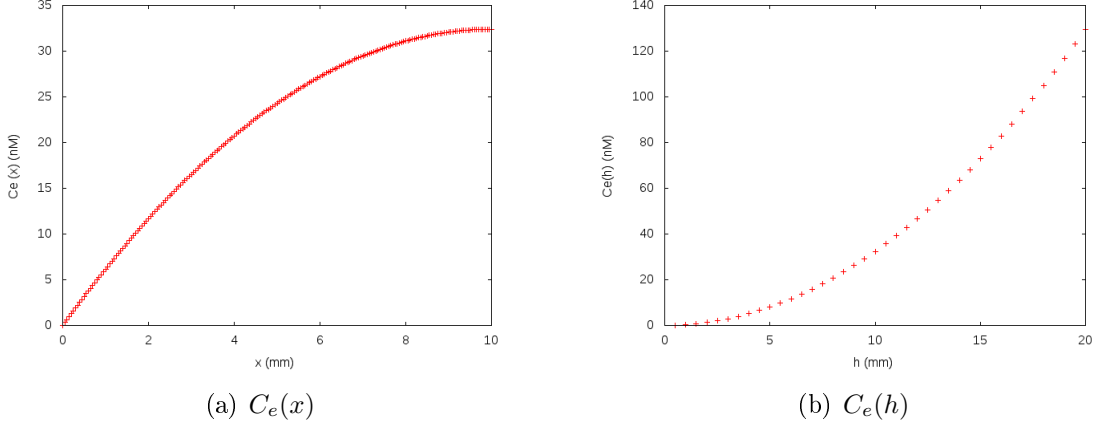
(a) $C_e(x)$

(b) $C_e(h)$

Figure 3.2: The first figure shows $C_e(x)$ at temporal equilibrium. The second figure shows $C_e(h)$ at temporal equilibrium. Parameters are $\rho_p = 10^8\ cell/l$, $\alpha = 7 \cdot 10^{-9}\ nMol/(cell \cdot h)$ and $k = 0.05\ h^{-1}$

The study at temporal equilibrium is very similar to that we discussed in chapter 2, in fact the equation is the same as well as the boundary conditions. Therefore the steady state solution of the second order differential equation as a function of x is

$$C_e(x) = C_0 \left[1 - \frac{cosh[\lambda(h - x)]}{cosh(\lambda h)} \right]$$

and as a function of h

$$C_e(h) = C_0 \left[1 - \frac{1}{cosh(\lambda h)} \right]$$

where

$$C_0 = \frac{\tilde{\alpha}\rho_p}{\tilde{k}} = \frac{\alpha}{kV_B}$$

and

$$\lambda = \sqrt{\frac{\tilde{k}}{D}} = \sqrt{\frac{k_M k}{k + k_M} \frac{V_B \rho_p}{D}}$$

In Figure 3.2 we can see $C_e(x)$ and $C_e(h)$ for an adequate choice of parameters. A huge difference from Model 0 is given by the fact that now the maximum reachable value of $C_e(h)$ does not depend on bacteria density. In fact this value is no other than C_0. This is not evident from Figure 3.2 since $C(h)$ has not reached equilibrium yet, but it is clear for a different choice of parameters and a coarse grained scale of h. An example of this behaviour can be seen in Figure 3.3.

Unfortunately the small length behaviour is mathematically the same as that found
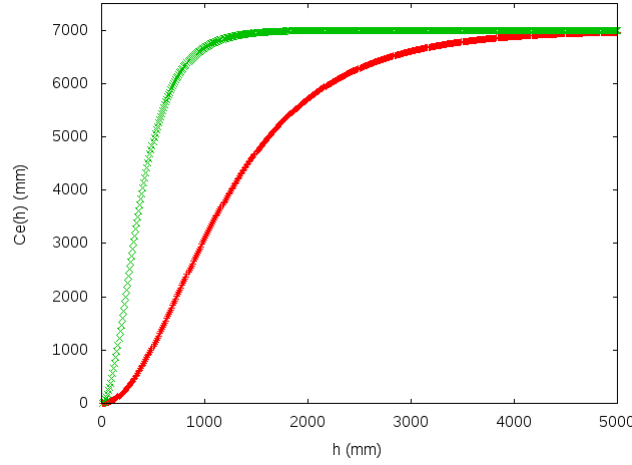
Figure 3.3: Parameters are $\alpha = 7 \cdot 10^{-9} \; nMol/(cell \cdot h)$, $k = 1000 \; h^{-1}$. The red curve reptesents $C(h)$ for a producers' density $\rho = 10^7 \; cell/l$ while the green curve for a producers' density $\rho = 10^8 \; cell/l$. The figure puts in evidence concentration is indipendent from bacterial density when $\frac{\partial C}{\partial t} = 0$ and $\frac{\partial^2 C}{\partial x^2}$.

in Model 0:

$$C_e(h) \simeq \frac{\tilde{\alpha}}{D} \rho_p h^2$$

This means that also the physical behaviour is the same. In particular it means that if we have two systems with the same α and the same k, but two different legnth h_1 and h_2, and two different densities ρ_1 and ρ_2, we got that

$$C_e(\rho_1, h_1) > C_e(\rho_2, h_2) \iff \frac{h_1}{h_2} > \sqrt{\frac{\rho_2}{\rho_1}}$$

Therefore, if we have a ratio of 10 in densities, which is the situation of our experimental study, we have

$$\frac{h_1}{h_2} > \sqrt{10} \simeq 3,16$$

which is not enough to explain the experimental result. In that case we found a ratio of 2.

One should argue that experimental data are not at temporal equilibrium. To check this possibility we numerically compute the non equilibrium solution using the FTCS scheme shown in section 1.4. The update formula is very similar to that of the Model 0, with just the substitution of α and k with the effective values.

In Figure 3.4 we can see the behaviour of $C(h)$ (for a suitable choice of parameters). Similarly to Model 0, non-equilibrium solution has the same behaviour as the

equilibrium one for small lengths. This means that both in the equilibrium and in the non-equillibrium case the new model is not giving any significant improvement to explain the experimental behaviour at short distances. Therefore this model has some interesting and relevant features, but it is not what we are exactly looking for.
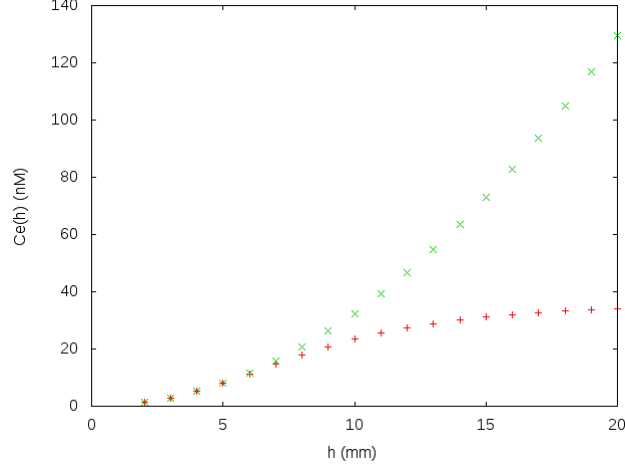

Figure 3.4: Sketch of $C_e(h)$. The green on is at time equilibrium, the red one is at $t = 50\ h$. Parameters are $\rho_p = 10^8\ cell/l$, $\alpha = 7 \cdot 10^{-9}\ nMol/(cell \cdot h)$, $k = 0,05\ h^{-1}$. Behaviour is the same for small lengths

3.1.2   The external chemical degradation

A way to further improve the model consists in adding an external chemical degradation, since AHL molecules can degrade inside bacteria cells, but can also do it in the external environment due to chemical reasons [10]. In such situation equations become

$$\begin{cases} \frac{\partial C_e}{\partial t} = D\frac{\partial^2 C_e}{\partial x^2} - k_M(C_e - C_p)\rho_p V_B - k_e C_e \\ \frac{\partial C_p}{\partial t} = \frac{\alpha}{V_B} - k_M(C_p - C_e) - kC_p \end{cases} \tag{3.3}$$

The model remains almost the same; it exhibits a difference in the definition of $\tilde{k}$, which now becomes:

$$\tilde{k} = \frac{k_M k}{k + k_M}\rho_p V_B + k_e$$

The value of the chemical degradation of AHL molecules in agar environment is given by [6] and is $k_e = 1/7\ days^{-1} = 5,95 \cdot 10^{-3}\ h^{-1}$. While its value k inside bacteria cells is not known. This simple redefinition of $\tilde{k}$ is of course not sufficient to significantly modify the previous model.

3.1.3 Producers, reporters and external environment

A further step to make the model more realistic consists in considering the difference between bacteria producing AHL and bacteria which report the presence of such molecules (see section 1.1.4). Hence we have three different environments instead of two, leading to equations:

$$\begin{cases} \frac{\partial C_e}{\partial t} = D\frac{\partial^2 C_e}{\partial x^2} - k_M(C_e - C_p)\rho_p V_B - k_M(C_e - C_r)\rho_r V_B \\ \frac{\partial C_p}{\partial t} = \frac{\alpha}{V_B} - k_M(C_p - C_e) - kC_p \\ \frac{\partial C_r}{\partial t} = -k_M(C_r - C_e) - kC_r \end{cases} \tag{3.4}$$

where C_r is the concentration of AHL molecules inside reporters. Just notice that we supposed the same degradation constant k both inside producers and inside reporters.

In the spirit of the prevoius section, we suppose a steady state equilibrium inside cells:

$$\frac{\partial C_p}{\partial t} = \frac{\partial C_r}{\partial t} = 0$$

The result is an analogous equation of 3.2, but again with a different definition of the effective degradation rate $\tilde{k}$, which now becomes

$$\tilde{k} = \frac{k_M k}{k + k_M}\rho_p V_B + \frac{k_M k}{k + k_M}\rho_r V_B$$

As stated at the end of the previous section, a redefinition of $\tilde{k}$ is not sufficient to obtain the desired behaviour for small lengths.

3.1.4 The Michaelis-Menten degradation

Another feature that can be introduced to make our model more realistic, is to suppose that degradation of AHL molecules inside bacteria is due to the presence of enzymes [7]. This means that we need to consider a degradation term of Michaelis-Menten type (see section 1.3). In other words

$$\frac{k_1 C}{k_2 + C}$$

where k_1 is the maximum velocity of the reaction and k_2 is the Michaelis-Menten constant.

Therefore, if we consider for simplicity just producers (and not reporters) and we neglect the chemical internal and external degradation, we obtain the system of equations:

$$\begin{cases} \frac{\partial C_e}{\partial t} = D\frac{\partial^2 C_e}{\partial x^2} - k_M(C_e - C_p)\rho_p V_B \\ \frac{\partial C_p}{\partial t} = \frac{\alpha}{V_B} - k_M(C_p - C_e) - \frac{k_1 C_p}{k_2 + C_p} \end{cases} \tag{3.5}$$

We can impose the equilibrium of internal concentration in order to find C_p as a function of C_e. This time, the situation is more complicated since we find a second grade equation, which, once solved, leads to the unique solution

$$C_p = \frac{-k_M k_2 V_B + k_M V_B C_e - k_1 V_B + \alpha + \sqrt{\Delta(C_e)}}{2 k_M V_B}$$

where

$$\Delta(C_e) = (-k_M k_2 V_B + k_M V_B C_e - k_1 V_B + \alpha)^2 + 4 k_M V_B (\alpha k_2 + k_M k_2 V_B C_e) > 0$$

We obtain a unique solution, since we have to impose the positive value of C_p. If we put this expression inside the differential equation for C_e, we obtain:

$$\frac{\partial C_e}{\partial t} = \frac{1}{2}(\alpha + \sqrt{\Delta(C_e)})\rho_p + D\frac{\partial^2 C_e}{\partial x^2} - \frac{1}{2}(k_M C_e + k_M k_2 + k_1)\rho_p V_B \qquad (3.6)$$

where we get, as usual, a production, a diffusion and a degradation term. This situation is more complicated and even in the steady state case we cannot find an analytical solution due to the presence of non linear terms. The only possibility is to find a numerical solution with the FTCS scheme. We do not write the numerical update formula, it can be obtained in the same way as that of Model 0 in chapter 2.

The case of total equilibrium [3] is very interesting, because it leads to a particular result. To find it, we need to solve the equation:

$$\frac{1}{2}(\alpha + \sqrt{\Delta(C_e)})\rho_p - \frac{1}{2}(k_M C_e + k_M k_2 + k_1)\rho_p V_B = 0$$

If we try to solve it in order to find the value of C_e, we obtain a very simple expression

$$C_e = \frac{\alpha k_2}{k_1 V_B - \alpha}$$

the positive value of concentration as physical quantity implies that the following condition must be imposed

$$k_1 V_B > \alpha$$

This is a necessary condition for the existence of the saturation value. If it is not satisfied, there is not a saturation value for C_e. It means that production is too strong and wins over degradation, letting a continuous increase of molecules concentration.

---

[3]with the expression total equilibrium we consider a situation in which $\frac{\partial C}{\partial t} = 0$ and $\frac{\partial^2 C}{\partial x^2} = 0$.

It is important to stress that if we let $k_1, k_2 \longrightarrow \infty$, in a way that the ratio $k_1/k_2 = k < \infty$, then

$$\frac{k_1 C_e}{k_2 + C_e} \longrightarrow k C_e$$

therefore the model returns to be the one with the internal chemical degradation coming from equation 3.1. Notice that a proof that this really happens is given by the fact that at total equilibrium C_e reaches the same value as that in the model described by equation 3.1.

We do not discuss in great detail this model, but we focus as usual on the system size dependence. In this case, we are not able to find an analytical solution, even for the steady-state case, therefore the size dependence study is more difficult. However we can study out of equilibrium numerical solutions in order to see if $C_e(h, t)$ follows a behaviour similar to the experimental one. Figure 3.5 shows that, for a suitable choice of parameters, the parabolic function perfectly fits numerical data for small lengths. This means that the change of degradation does not influence size dependence. This model results to be more complicated to study but it adds a more complete descritpion of the degradation. However it seems not so relevant in order to decribe size dependence.
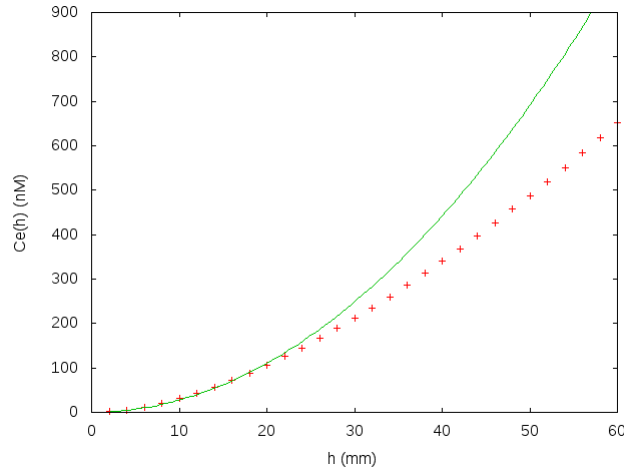

Figure 3.5: Graphs of $C_e(h)$ with a parabolic fit. Parameters are $\rho_p = 10^8 \; cell/l$, $\alpha = 7 \cdot 10^{-9} \; nMol/(cell \cdot h)$, $k_1 = 1 \; nM/h$, $k_2 = 1 \; nM$. Fit is performed in the interval $[0 : 20]$ and gives the function $f(h) = (0,276 \pm 0,004)h^2$.

3.2 The Flux Model

In our model a possible source of mistake in our model might be the choice of boundary conditions. Up to now we have assumed that the boundary between

cylinders and agar is completely absorbing. In this section we remove this hypothesis and we investigate the possibility that AHL molecules flow out with a constant flux. This means that the reservoir is not able to completely absorb molecules but it can do that only with a fixed rate: an hypothesis that seems to be physically reasonable. Therefore, for different lenghts of the system, we have a fixed flux J of particles which go out through the boundary in $x = 0$. The most important consequence of this model is that generally $C(0) \neq 0$.

So, let's consider Model 0, therefore equation 2.5:

$$\frac{\partial C(x,t)}{\partial t} = \alpha\rho + D\frac{\partial^2 C(x,t)}{\partial x^2} - kC(x,t)$$

The boundary condition in $x = h$ is reflecting as usual, so

$$\frac{\partial C(x,t)}{\partial x}\Big|_{x=h} = 0$$

As we have already said, the change is in the absorbing boundary in $x = 0$. If we consider the First Fick's Law 1.1 we got that the derivative of concentration is linked to the flux of particles by the following relation:

$$\frac{\partial C(x,t)}{\partial x}\Big|_{x=0} = \frac{J}{D}$$

where a double minus sign must be considered in this relation, one coming from the Fick's Law, and the other coming from the fact that we are considering the flux of particles towards the negative direction of the x axis.

The initial condition is the same as the previous studies:

$$C(0) = 0 \ \forall x$$

To find the time equilibrium solution, we need to solve the same equation as that in Model 0, but with a different boundary condition. Its solution is:

$$C(x) = \frac{\alpha\rho}{k} - \frac{J}{\lambda D}\left[\frac{cosh(\lambda(x - h))}{sinh(\lambda h)}\right]$$

and in function of the lanes' length h

$$C(h) = \frac{\alpha\rho}{k} - \frac{J}{\lambda D}\frac{1}{sinh(\lambda h)}$$

This latter is an increasing function in h, which tends to the maximum value
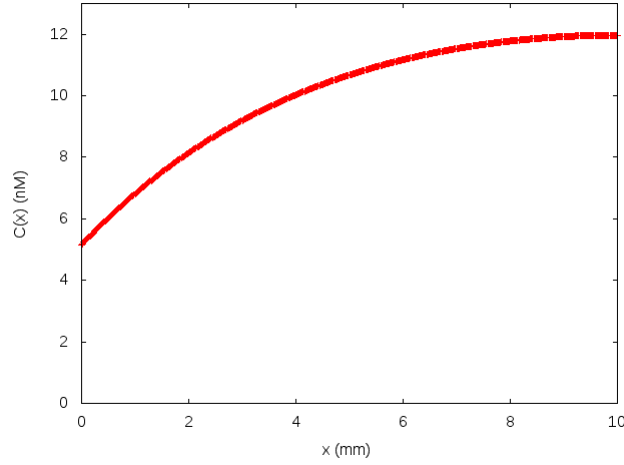
$$C(\infty) = \frac{\alpha\rho}{k}$$

Figure 3.6: Graph of $C_e(x)$. Parameters are $\rho_p = 10^8 cell/l$, $\alpha = 7 \cdot 10^{-9} nMol/(cell \cdot h)$, $k = 0,05\ h^{-1}$, $J = 2nM/h$. In this model we can obtain $C(0) \neq 0$ as shown in figure.

An example of $C(x)$, when $C(0) \neq 0$, is shown in Figure 3.6.
In this case we could have physically meaningless results, since $C(x)$ could mathematically have negative values. This problems can be solved just making some hypotheses only on $C(0)$ (since $C(x)$ is an increaing function of x). If we compute the concentration of signal molecules in the boundary $x = 0$, we obtain:

$$C(0) = \frac{\alpha \rho}{k} - \frac{J}{\lambda D} \frac{1}{tgh(\lambda h)}$$

hence we have a first positive term which is fixed once parameters are chosen and a second term which depends on the length h through the hyperbolic tangent (supposing that J is fixed). Remembering $tgh(x)$ behaviour, we have

$$tgh(\lambda h) \in [0, 1] \rightarrow \frac{1}{tgh(\lambda h)} \in [1, \infty]$$

Therefore the second term has a minimum value given by $J/\lambda D$ and no maximum value. This means that we could have two possible behaviours on the basis of the choice of the parameters:

1. The minimum value of the second term is smaller than the first term, therefore we have a range of length $h \in]0, h^*[$ where $C(0) < 0$, we reach then a critical h^* where $C(0) = 0$ and for $h \in]h^*, \infty[$ we have $C(0) > 0$.

2. The minimum value of the second term is bigger than the first term, thus the value of $C(0)$ is always negative (for every value of h).

Being in case 1. or 2. depends on the minimum value of the second term; hence the condition to be in 1. is

$$\frac{\alpha\rho}{k} - \frac{J}{\lambda D} > 0 \;\to\; J < \frac{\alpha\rho}{\lambda}$$

Physically speaking, the situation $C(0) < 0$ is meaningless, since concentration is a positive physical quantity. Therefore, we need to fix a constraint. The most reasonable idea is to suppose that the flux J remains fixed when $C(0) > 0$ and then it adapts its value under the critical length h^* in a way that $C(0) = 0$ for all lengths below the critical one. This latter assumption means that the system returns to be Model 0 under the critical length. Therefore we obtain:

1. $\exists\, h^* \mid C(0) = 0$
It means that the minimum value of the second term is smaller than the first term. In other words, we can find a length which satisfies

$$C(0) = \frac{\alpha\rho}{k} - \frac{J}{\lambda D}\frac{1}{tgh(\lambda h^*)} = 0$$

which means

$$h^* = \frac{1}{\lambda}tgh^{-1}\left(\frac{J\lambda}{\alpha\rho}\right)$$

The existence of this length has as a concequence that
for $h > h^*$: $C(0) > 0$ and J has the fixed chosen value.
for $h < h^*$: $C(0) = 0$ and $J = \frac{\alpha\rho}{\lambda}tgh(\lambda h)$
In Figure 3.7 we can see this double behaviour. The plot shows $C(h)$ which is a countinuous function in h^* (but its derivative is not continuous).

2. $\nexists\, h^* \mid C(0) = 0$
It means that the minimum value of the second term is greater than the first term, or in other words that
$$\frac{\alpha\rho}{k} - \frac{J}{\lambda D}\frac{1}{tgh(\lambda h)} < 0 \;\forall h$$

This condition leads the system to be always the same as Model 0: the value of J is too high for these choices of parameters, hence its value must always be the one of Model 0 ($C(0) = 0\; \forall h$). In this situation we gain nothing by this new model.

We examine now what happens Model 0 until the value of h^* and something new beyond it.
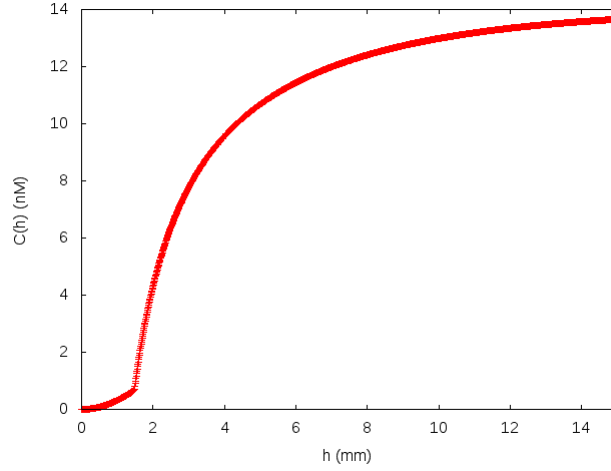
Figure 3.7: Graph of $C_e(h)$. Parameters are $\rho_p = 10^8$ $cell/l$, $\alpha = 7 \cdot 10^{-9}$ $nMol/(cell \cdot h)$, $k = 0,05$ h^{-1}, $J = 1$ nM/h. The hybrid behaviour is evident.

Our hope is to find a new length dependent behaviour with this hybrid model. We therefore define $\overline{C}$ as

$$\overline{C} = \begin{cases} \frac{\alpha\rho}{k} - \frac{J}{\lambda D}\frac{1}{sinh(\lambda\overline{h})} & if\ \overline{h} > h^* \\ \frac{\alpha\rho}{k}\left[1 - \frac{1}{cosh(\lambda\overline{h})}\right] & if\ \overline{h} < h^* \end{cases}$$

We fix a particular value of $\overline{C}$ and starting from fixed values for α and k, we then calculate for a given ρ_1 the critical length h_1^*. After that we invert the relation above in order to calculate the $\overline{h_1}$ relative to that value of concentration (being aware if we are above o below the critical length value). Then we repeat the same calculation for another bacteria density ρ_2 in order to find $\overline{h_2}$. We finally calculate the ratio $\overline{h_2}/\overline{h_1}$ in order to see the size dependence. This procedure is easily understable in Figure 3.8.
The idea is to fix a value $\overline{C}$ at around nM, to set $\rho_1 = 10^7 cell/l$ and $\rho_2 = 10^8 cell/l$ and to analyze the size dependence. The values of α and k are then spanned over different orders of magnitude in order to see if there's a set of values which gives a result compatible with experimental findings.
Results are not so sastisfying. If we are interested only in the region of the new behaviour $(h > h^*)$, we get

$$\frac{h_1}{h_2} \simeq 10$$

which is a very high value.
On the other hand, if we focus on the total hybrid model, we got again
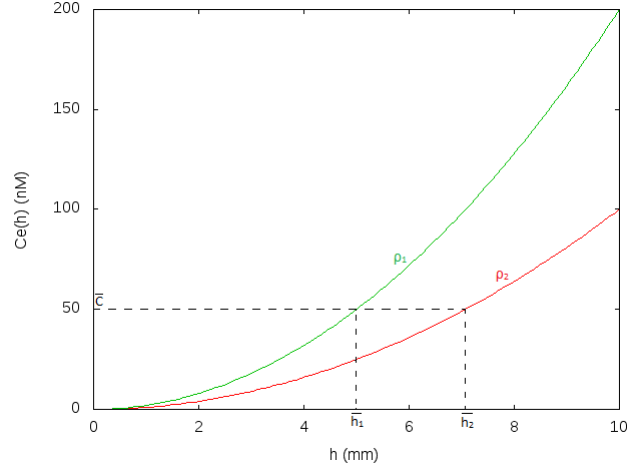
$$\frac{h_1}{h_2} \simeq 3,3$$

Figure 3.8: Red and green functions represent two different $C_e(h)$. In particular they only differ from the density of producers. We can suppose to fix C_e and see at which length these two systems reach this concentration. In this way we can calculate the ratio of the two lengths.

which is the same ratio obtained for Model 0, which is not sufficient to explain experimental results.

Therefore, this hybrid model does not give better results than Model 0, but it is much harder to manage.

3.3   The chosen model and results

In the previous sections we introduced several models. Each one of them stressed different aspects of the biological problem that we want to address. Unfortunately, none of them is able to predict the results of our experiment. It is then necessary to consider the complex biological cascade and chemical reactions which are triggered by AHL, in order to explain the coloured material observed in the experiment.

Before going to describe this part in the next chapter, we need to decide which model is more suitable to describe diffusion of AHL. Our choice falls in the inside-outside model which uses three different environments (producers, reporters and exterior) with AHL chemical degradation both inside and outside bacteria. This seems to be the more realistic model and it is also not very complicated to study. Let's rewrite the equations of the model and the update formula for the numerical

solution:

$$
\begin{cases}
\frac{\partial C_e}{\partial t} = D\frac{\partial^2 C_e}{\partial x^2} - k_M(C_e - C_p)\rho_p V_B - k_M(C_e - C_r)\rho_r V_B - k_e C_e \\
\frac{\partial C_p}{\partial t} = \frac{\alpha}{V_B} - k_M(C_p - C_e) - kC_p \\
\frac{\partial C_r}{\partial t} = -k_M(C_r - C_e) - kC_r
\end{cases}
\tag{3.7}
$$

with boundary conditions

$$
\begin{cases}
C_e(x,t)|_{x=0} = 0 & \text{Absorbing condition} \\
\frac{\partial C_e(x,t)}{\partial x}|_{x=h} = 0 & \text{Reflecting condition}
\end{cases}
$$

and initial conditions

$$
C_e(x,0) = C_p(x,0) = 0 \; \forall x
$$

We need to specify that the rate of chemical degradation inside producers and reporters is k which is not a known value, while that one in the external agar environment is $k_e = 1/7 \; days^{-1}$.

These equations, supposing temporal equilibrium inside producers and reporters, lead to

$$
\frac{\partial C_e}{\partial t} = \tilde{\alpha}\rho_p + D\frac{\partial^2 C_e}{\partial x^2} - \tilde{k}C_e
\tag{3.8}
$$

where

$$
\tilde{\alpha} = \frac{\alpha k_M}{k + k_M}
$$

$$
\tilde{k} = \frac{k_M k}{k + k_M}\rho_p V_B + \frac{k_M k}{k + k_M}\rho_r V_B + k_e
$$

where $k_M = 180 \; h^{-1}$, $V_B = 10^{-15} \; l$ and $\rho_r = 10^{11} \; cell/l$.

Its numerical solution is

$$
C_e[i][j+1] = C_e[i][j] + \tilde{\alpha}\rho_p \Delta t + \frac{D\Delta t}{\Delta x^2}(C_e[i+1][j] - 2C_e[i][j] + C_e[i-1][j]) - \tilde{k}\Delta t C_e[i][j]
$$

where i is the spatial index and P the number of spatial intervals:

$$
i \in [0, P] \longrightarrow x = i\Delta x = \frac{ih}{P} \in [0, h]
$$

and j is the temporal index and M the number of spatial intervals:

$$
j \in [0, M] \longrightarrow t = j\Delta t = \frac{jt_{MAX}}{M} \in [0, t_{MAX}]
$$

with inital conditions

$$
C_e[i][0] = 0 \; \forall i \in [0, P]
$$

and boundary conditions

$$\begin{cases} C_e[0][j] = 0 & \forall j \in [0, M] \text{ Absorbing condition} \\ C_e[P][j] = C_e[P-1][j] & \forall j \in [0, M] \text{ Reflecting condition} \end{cases}$$

At first, we are interested in computing $C_e(h, t)$, this means considering $C_e[P][j]$ for a given length h.

Since Quorum Sensing trigger takes place inside reporters, we need to consider C_r. Therefore once obtained C_e we are able to calculate it as

$$C_r = \frac{k_m}{k + k_m} C_e$$

This last relation is clearly an approximation, since it comes from the internal equilibrium condition.

In this study we have two parameters which are not fixed: α and k. At first, we find a range for α in order to have a concentration inside reporters around $1 \div 10 \ nM$ at $\rho_p = 10^7 \ cell/l$. Since the main role of α, being a rate of production, is to determine the order of magnitude of AHL concentration. Then, we span over different order of magnitude of α and k in order to find suitable values which let the approach to experimental data. Similarly to what we made in the section of the flux model, the idea is to find a low value for the ratio h_1/h_2 once chosen a certain value for C_e (it's easier fixing C_e rather than C_r; as we see they will not be so different).

In the spanning we found an acceptable value for our two parameters $\alpha = 7 \cdot 10^{-9} \ nMol/(cell \cdot h)$ and $k = 0,05 \ h^{-1}$. The value of α is often uncertain, since in different QS systems it could vary over different orders of magnitudes. However this value is not so far as that found in other works as [6] and [17]. The value of the chemical degradation rate k inside bacteria cells is ten times the value in agar (k_e), therefore it also could be reasonable, since the presence of enzymes should enhance degradation. Morevorer we can notice that for this value of k we have as a concequence $C_r \simeq C_e$. It is a very important particular that will let us to focus on the external concentration instead of C_r and that will let us to apply a useful approximation in the following chapter.

The values of $C_e(h, t)$ and our experimental results are shown in Figure 3.9. It seems that the Quorum Sensing threshold is around $C^* = 1,7 \ nM$. Again, it is a reasonable value consistent with literature [16]. Our theoretical results are not so bad, since the first two columns agree with experiments. What is not in accordance with experimental data is the behaviour at small lengths of the columns with densities $\rho_p = 10^8 \ cell/l$ and $\rho_p = 10^9 \ cell/l$. Their concentration seems to be too strong, in particular in the last two columns. This is probably the cause

Experimental Results

Height (cm)	$\rho_p = 10^7$ cell/l		$\rho_p = 10^8$ cell/l		$\rho_p = 10^9$ cell/l	
	$t = 24\,h$	$t = 92\,h$	$t = 24\,h$	$t = 92\,h$	$t = 24\,h$	$t = 92\,h$
0,2						
0,4						
0,6						
0,8						
1,0						
1,2						
1,4						
1,6						
1,8						
2,0						

Theoretical Results

Height (cm)	$\rho_p = 10^7$ cell/l		$\rho_p = 10^8$ cell/l		$\rho_p = 10^9$ cell/l	
	$t = 24\,h$	$t = 92\,h$	$t = 24\,h$	$t = 92\,h$	$t = 24\,h$	$t = 92\,h$
0,2	0.126595	0.126595	1.26595	1.26595	12.6595	12.6595
0,4	0.48543	0.493086	4.8543	4.93086	48.543	49.3085
0,6	0.90567	1.06222	9.0567	10.6222	90.567	106.222
0,8	1.20285	1.76241	12.0285	17.6241	120.285	176.240
1,0	1.37786	2.47141	13.7786	24.7141	137.786	247.140
1,2	1.47346	3.09088	14.7346	30.9088	146.346	309.088
1,4	1.52267	3.58801	15.2267	35.8801	152.267	358.801
1,6	1.54653	3.96942	15.4653	39.6942	154.653	396.942
1,8	1.55742	4.25467	15.5742	42.5467	155.742	425.466
2,0	1.56208	4.46428	15.6208	44.6428	156.208	446.427

Figure 3.9: Experimental and theoretical results considering only AHL molecules dynamics. Blue values mean that those cylinders are supposed to be "on". Values in the table are AHL concentrations in nM.

(and the consequence) of the fact that we could not find a better dependece on h. Another problem is given by the fact that we are not able to build a scale of "turning on", but just to say "on" or "off".

In the following chapter we will improve the study, focusing on the remaining part of the dynamics induced by AHL concentration. This study will be crucial in the explanation of the experiment.

Chapter 4

Models for the Quorum Sensing response

Up to now we have only studied dynamics concerning AHL signal molecules, especially their diffusion. But if we look at the system that we want to model, we realize that this is just a small part of the entire process. In fact the entire dynamics can be divided (in first approximation) in three different steps:

1. AHL signal molecules dynamics: their production, diffusion and degradation.

2. Trigger of Quorum Sensing mechanism: when the threshold concentration of signal molecules is reached, they bind to the TraR protein, which activates the transcription of the gene encoding for the production of β-Gal enzyme.

3. β-Gal and X-Gal dynamics: β-Gal enzyme, which is produced after the trigger of QS, binds to X-Gal, hydrolizing it, and then the product spontaneously dimeryzes and is oxidized in presence of oxygen.

The aim of this chapter is to find a model to describe these three diffrent steps which presumably are the ingredient we are looking for to explain our experimental results. Our expectation is to be able to fit in a good way the experimental results found in section 2.2.
Therefore in the first part of the chapter we describe how to model the central Quorum Sensing mechanism, which is a link between signal molecules concentration and β-Gal enzyme production. Then, we focus on the dynamics concerning the hydrolization of X-Gal and its successive processes in order to arrive to the final coloured product, which is what we really observe. As we will see, in this last part an important role is played by the diffusion of X-Gal and its products. At the end of the chapter, we will exhibit our results comparing them with experiments.

4.1   Trigger of Quorum Sensing mechanism

The first process that we need to model is the heart of Quorum Sensing. Until the concentration of molecules is low, β-Gal is not produced and we don't see any coloured product. But when threshold of Quorum Sensing is reached, AHL molecules bind to the regulatory protein TraR, which acts as a transcriptional factor (TF). This complex ties to the promoter of the gene *lacZ:traG* in the DNA, activating its trascription [24]. The role of this gene is to encode for production of the β-Gal enzyme.

What we have just described is the entire process that links the dynamics of signal molecules to that of the X-Gal substrate. Therefore it is a sort of link between the two major dynamics which take place in this system.

We do not consider the entire microbiological and genetic process underlying this mechanism, as other authors do, but we merely focus on the reception of signal molecules and the subsequent enzyme production. Hence, we think that the main feature is the following: m molecules of AHL are necessary to trigger the genetic process which leads in a certain way to the enzime production. In other works, for example, authors prefer to concentrate on how the TF is able to reach the gene promoter on DNA [14] or how the QS regulatory mechanism works in detail [13]. Therefore, let's suppose at first to have a transcriptional factor having m binding sites. This protein T_- is initially inactivated, but when m signal molecules fill its sites, it turns into the activate state T_+. This number m has a clear physical meaning given by the structure and the function of the TF, but unfortunately (as in our case) is not yet known and its value has to be guessed by interpolating experimental data. The activated TF is then what generates the activation of the enzyme production in our model. We can write the activation of the TraR protein as a chemical reaction [20]:

$$mAHL + T_- \underset{k_-}{\overset{k_+}{\rightleftharpoons}} T_+$$
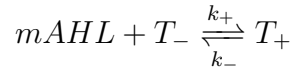
Let's indicate concentrations of these quantities with the notation $[\cdot]$. They are functions of space and time since AHL concentration depends on them. In particular then, let's remember that $[AHL](x,t) \equiv C_e(x,t)$, given by the fact that $C_r \simeq C_e$ (for our value of k). For simplicity of notation, we do not write the variables dependence. Hence we are able to write the variation of T_+ concentration in respect to time as

$$\frac{\partial[T_+]}{\partial t} = k_+ C_e^m [T_-] - k_-[T_+]$$

This scheme specifies an equilibrium condition

$$\frac{[T_+]}{[T_-]} = \frac{k_+}{k_-} C_e^m = \frac{C_e^m}{k_m}$$

where

$$k_m = \frac{k_-}{k_+}$$

is a compound dissociation constant at equilibrium, which reflects the "concerted binding" of all m ligands. The reciprocal of the dissociation constant is often used and it is called association constant. They are a sort of ligand affinity measure. In this type of study, the dissociation constant is written in the form $k_m = a^m$ where a is called Hill's constant. Later on we will see its meaning.

We are now able to write the function f which represents the fraction of activated transcriptional factors in respect to the total:

$$f = \frac{[T_+]}{[T_+] + [T_-]} = \frac{[T_+]/[T_-]}{[T_+]/[T_-] + 1} = \frac{C_e^m/a^m}{C_e^m/a^m + 1} = \frac{C_e^m}{C_e^m + a^m}$$

and in function of its variables

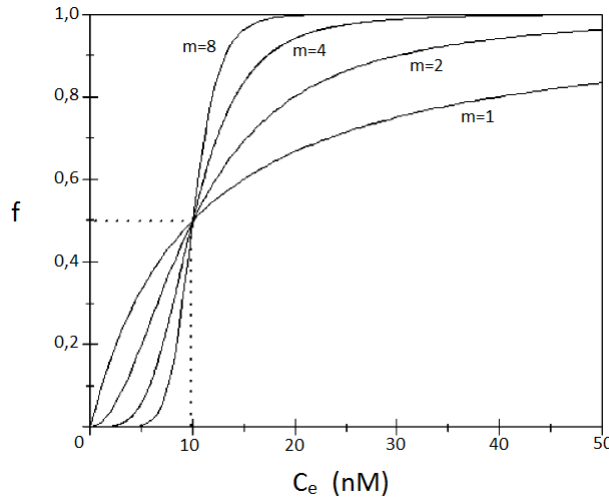$$f(x,t) = \frac{C_e^m(x,t)}{C_e^m(x,t) + a^m} \tag{4.1}$$

Figure 4.1: Sketch of f. Hill's constat is set as $a = 10$

This is often referred as Hill Equation. A plot of f has a sigmoidal character when $m > 1$, as we can see in Figure 4.1. This implies that the curve is steeper in the middle than at the start. Moreover in the figure we can see that f gives values from 0 to 1 and that growing values of m give a more rapid behaviour of f.

The mathematical role of a is perfectly clear now, in fact it represents the concentration at which $f(x,t) = 1/2$. But it has also a fondamental role if we focus on

its meaning in biological physics. If we imagine that more than half of activated transcriptional factors means that Quorum Sensing has been activated, then we can explain a as the QS threshold. With this statement we want to say that a represents the value of signal molecules concentration at which Quorum Sensing is triggered. Its value for this type of QS is around nM [6]. If we look at Figure 3.9, we can suppose that $a = 1,7\ nM$, since from experimental data we can assert that Quorum Sensing trigger for $\rho_p = 10^7\ cell/l$ at $t = 92\ h$ is at the length of $8\ mm$. The choice we make is not very precise, but it is phisically and biologically reasonable. For the following study, we realized the best results are obtained with $m = 1$.

We have just exhibited the process of activation of regulatory proteins. The next step is to decide how to model the production of β-Gal enzyme, which will be indicate by E. The idea comes from [12]: we need to describe how much E is produced in time unit for a given fraction of activated proteins. We can simply write it as

$$\frac{\partial [E]}{\partial t}(x,t) = Af(x,t)$$

where $[E]$ represents the enzyme's concentration. A is the maximum activity of regulatory proteins, or in other words how much E is made if every T_- has been activated in a particular position x.

Therefore the final result is

$$\frac{\partial [E]}{\partial t}(x,t) = A\frac{C_e^m(x,t)}{C_e^m(x,t) + a^m} \tag{4.2}$$

This is the equation which links signal molecules dynamics to X-Gal dynamics. We have omitted all the microbiology standing inside this process, because we hope to have a good description of experimental data with just a simple model. Investigating all the intermediate processes could dramatically complicate our model. We are now ready to face the last part of our study.

4.2 β -Gal and X-Gal dynamics

β-Gal enzyme is the direct result of Quorum Sensing mechanism in mutant *Agrobacterium tumefaciens* NTL4. When β-Gal can be found in the environment, it means that QS took place. The main question is how we can detect the presence of this enzyme. Exploiting the property that it hydrolizes the β-glycosidic bond formed between a galactose and its organic moiety, we introduced in our experiment an X-Gal substrate which is formed by galactose. Therefore the enzyme attaches to X-Gal and hydrolizes it. After that, the product of hydrolization spontaneously dimerizes and then it is oxidized in presence of oxygen. The final substance is
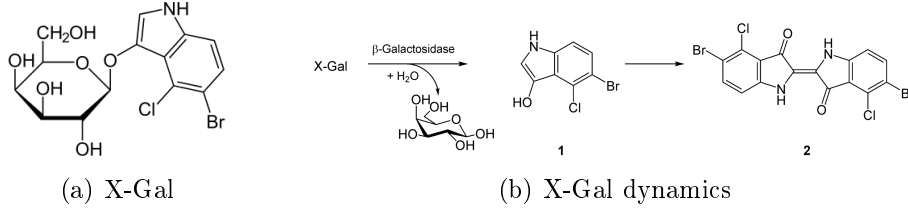
(a) X-Gal   (b) X-Gal dynamics

Figure 4.2: The first figure shows the structure of the X-Gal molecule, while the second one the reaction of hydrolization and dimerization + oxidiation of X-Gal.

blue coloured and can therefore be seen. In this section our aim is to try to model this process. Before proceeding, we are allowed to make an approximation. Since $C_e \simeq C_r$, in this subsequent dynamics we can suppose to avoid the space division between producers, reporters and exterior for β-Gal and X-Gal and therefore consider just one environment. This choice makes the following equations a little bit easier to study and solve. In figure 4.2 we propose again the scheme of the reaction that we need to model.

At first we need to stress that in our description, we will look always at the reflecting boundary $x = h$ of the lane.

Let's suppose at the beginning that we are able to see the product of the hydrolization process and hence we do not take in account of the dimerization+oxidation part. The reaction which takes place is the following:

$$E + S \underset{k_{-1}}{\overset{k_1}{\rightleftharpoons}} ES \overset{k_2}{\longrightarrow} E + P$$
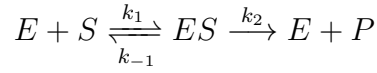
It describes the attachment of free β-Gal enzyme E to X-Gal substrate S, they form a bound state ES and then the result is a product P and again the free enzyme E. In our experiment the initial concentration of X-Gal is $[S_0] = 60 \ \mu g/ml = 146,83 \ \mu M$. The second result is obtained through its molar mass.

In biological physics when we treat an enzimatic reaction like the one written above, the Aldein hypothesis is often introduced in order to simplify dynamics. It consists in supposing that ES state is stationary, which means that $\partial[ES]/\partial t = 0$. However this hypothesis is consistent if we need to describe a system in which the total enzyme concentration $[E_T] = [E] + [ES]$ is constant. In fact in Figure 4.3 we can see a numerical solution of the equations describing this type of system and we can notice that $[ES]$ is constant until we do not consider very short times or the time interval in which the substrate S is totally consuming. The Aldein hypothesis can not be used in our system, since enzyme is continuously produced by bacteria once QS threshold has been reached and hence its total concentration does not remain constant. If we suppose a production of the type 4.2, we obtain a sketch similar to that in Figure 4.4. We are not allowed to consider ES as a
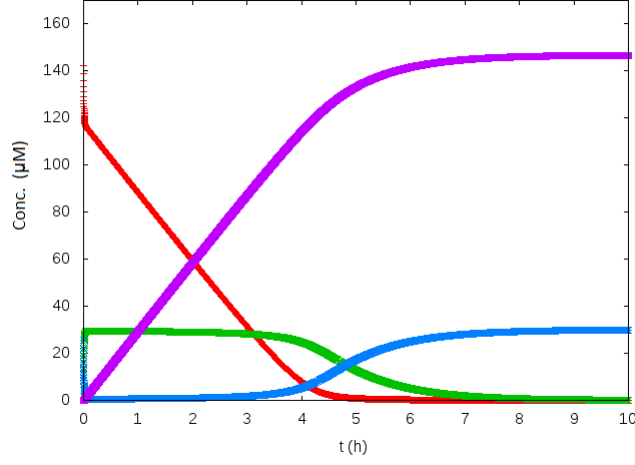
Figure 4.3: System with a constant concentration of total enzyme E_t. Red curve represents $[S]$, Green curve $[ES]$, Blue curve $[E]$, Violet curve $[P]$. Parameters are $k_1 = k_{-1} = k_2 = 1\ h^{-1}$, $A = 1\ nM/h$, , $[S_0] = 146, 83\ nM$.

steady state.

We have not written yet equations governing the evolution of enzyme and X-Gal concentration because there's a last ingredient lacking: diffusion. In fact we noticed by experiments that our system is not "turned on" at very small lenghts, no matter what producers density we consider. Models for AHL dynamics lack in a good explaination of this behaviour for high producers densities as we can see in Figure 3.9. We can suppose that this effect is probably given by diffusion of X-Gal, which is able to escape through the absorbing boundary before it can be hydrolized. Therefore, in our system we introduce diffusion of X-Gal substrate S and its product P. Since β-Gal enzyme is much bigger than X-Gal, we suppose it as fixed.

We are now able to write the differential equations governing our system. They firstly take in account of the chemical reaction, then diffusion is introduced together with the fact that free β-Gal enzyme is continuously produced (see equation 4.2). As result we obtain the following equations:

$$
\begin{aligned}
\frac{\partial [E]}{\partial t} &= Af(x,t) - k_1[S][E] + k_{-1}[ES] + k_2[ES] \qquad (4.3)\\
\frac{\partial [S]}{\partial t} &= -k_1[E][S] + k_{-1}[ES] + D\frac{\partial^2 [S]}{\partial x^2}\\
\frac{\partial [ES]}{\partial t} &= k_1[E][S] - k_{-1}[ES] - k_2[ES]\\
\frac{\partial [P]}{\partial t} &= k_2[ES] + D\frac{\partial^2 [P]}{\partial x^2}
\end{aligned}
$$

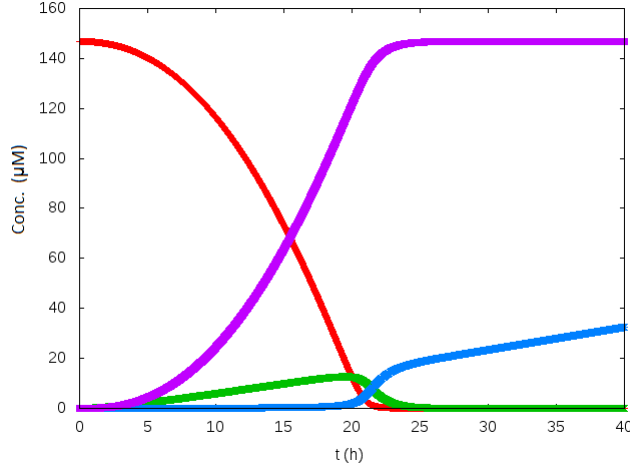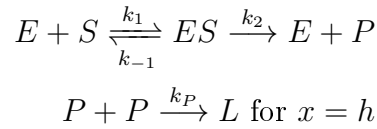Figure 4.4: System with a constant production of free β-Gal enzyme. Red curve represents $[S]$, Green curve $[ES]$, Blue curve $[E]$, Violet curve $[P]$. Parameters are $k_1 = k_{-1} = k_2 = 1\ h^{-1}$, $A = 1\ nM/h$, $[S_0] = 146,83\ nM$, $\rho_p = 10^8\ cell/l$, $\alpha = 7 \cdot 10^{-9}\ nMol/(cell \cdot h)$, $k = 0,05\ h^{-1}$

An example of sketch of this equations system can be observed in Figure 4.5. Diffusion effects are evident, since the product P reaches a maximum (smaller than $[S_0]$) and then it slowly diminishes and substrate S decreases in a more rapid way than without diffusion.

We can complete this model considering the next step, which means introducing dimerization+oxidation of the hydrolized product. This reaction consists in the fusion of two P molecules with the addition of an oxygen atom. This last fact implies that it can take place only in presence of oxygen, hence only in the reflecting boundary, because that is the only part of the system in contact with air. Therefore, in the second case reactions are

$$E + S \underset{k_{-1}}{\overset{k_1}{\rightleftharpoons}} ES \overset{k_2}{\longrightarrow} E + P$$

$$P + P \overset{k_P}{\longrightarrow} L \text{ for } x = h$$

This means that their differential equations can be written in the form

$$\frac{\partial [E]}{\partial t} = Af(x,t) - k_1[S][E] + k_{-1}[ES] + k_2[ES]$$

$$\frac{\partial [S]}{\partial t} = -k_1[E][S] + k_{-1}[ES] + D\frac{\partial^2[S]}{\partial x^2}$$

$$\frac{\partial [ES]}{\partial t} = k_1[E][S] - k_{-1}[ES] - k_2[ES]$$
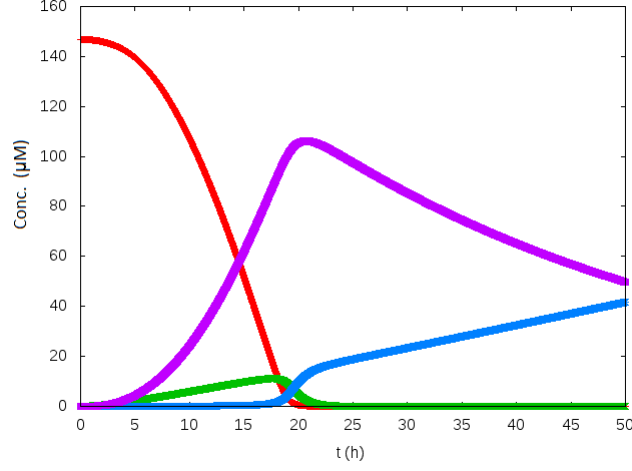
Figure 4.5: System with a constant production of free β-Gal enzyme and possible diffusion of X-Gal and its product. Red curve represents $[S]$, Green curve $[ES]$, Blue curve $[E]$, Violet curve $[P]$. Parameters are $k_1 = k_{-1} = k_2 = 1\ h^{-1}$, $A = 1\ nM/h$, $[S_0] = 146,83\ nM$, $\rho_p = 10^8\ cell/l$, $\alpha = 7 \cdot 10^{-9}\ nMol/(cell \cdot h)$, $k = 0,05\ h^{-1}$.

$$\begin{cases} \frac{\partial[P]}{\partial t} = k_2[ES] + D\frac{\partial^2[P]}{\partial x^2} & \text{if } x \neq h \\ \frac{\partial[P]}{\partial t} = k_2[ES] - k_P[P]^2 + D\frac{\partial^2[P]}{\partial x^2} & \text{if } x = h \end{cases}$$

$$\begin{cases} \frac{\partial[L]}{\partial t} = D\frac{\partial^2[L]}{\partial x^2} & \text{if } x \neq h \\ \frac{\partial[L]}{\partial t} = k_P[P]^2 + D\frac{\partial^2[L]}{\partial x^2} & \text{if } x = h \end{cases} \tag{4.4}$$

It is important to notice that the final product L can diffuse, since it is a small molecule as P and S are. With this improvement we have introduced a point with particular privileges ($x = h$) since the production of L only takes place there. This fact makes the study harder, due to the importance which space discretization assumes. An example of this behaviour is shown in Figure 4.6.

This model contains several free parameters which we need to determine. In particular they are A, k_1, k_{-1}, k_2, k_P. In the next section we will try to find them, and we will see the results emerging from this model. We anticipate that they will be in good accordance with experiments.

4.3   Results

After the theoretical discussion of the model that we think suitable for the description of experimental data, we need now to determine free parameters. The idea is therefore trying to span parameters values over different order of magnitudes
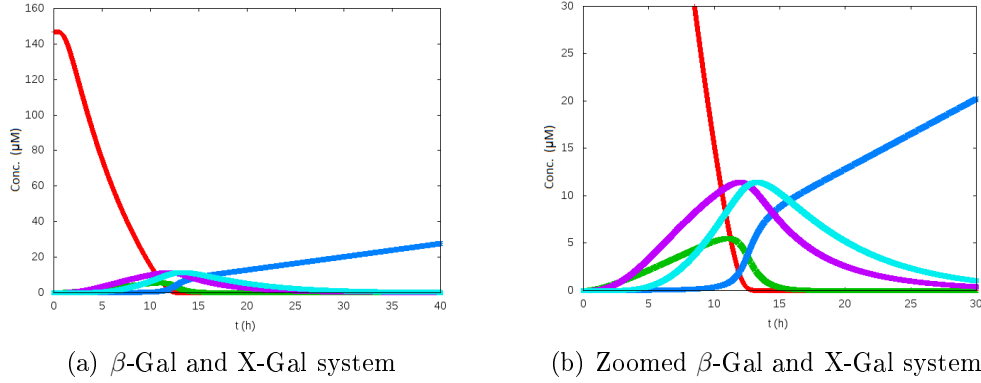
(a) β-Gal and X-Gal system

(b) Zoomed β-Gal and X-Gal system

Figure 4.6: System with a constant production of free β-Gal enzyme and possible diffusion of X-Gal and its products. Final process of dimerization+oxidation is also included. The second figure is the zoomed version of the first one. Red curve represents $[S]$, Green curve $[ES]$, Blue curve $[E]$, Violet curve $[P]$, light blue curve $[L]$. Parameters are $k_1 = k_{-1} = k_2 = k_p = 1\ h^{-1}$, $A = 1\ nM/h$, $[S_0] = 146,83\ nM$, $\rho_p = 10^8\ cell/l$, $\alpha = 7 \cdot 10^{-9}\ nMol/(cell \cdot h)$, $k = 0,05\ h^{-1}$.

to see if some of them are good to give results in accordance with experiments. Since diffusion has a big role in this model, we impose conditions linked to the fact that we want a final product's concentration for $h = 20\ mm$, $t = 24\ h$ and the lowest producers density, bigger than that found for very small lengths, for higher densities and/or later times. In particular we can use Figure 4.7 (which shows experimental data) to understand which constraints we decide to impose. We ask that $A < B$, $A < C$ and $A < D$ and therefore we look for parameters suitable with these choices. We impose only three conditions due to computational difficulties. As we will see by results, the first two conditions can be satisfied for particular choices of parameters, while the third one can never be satisfied, since diffusion has a too strong role.

Figure 4.7: Experimental data with marks on the lanes used for imposing conditions

We exhibit here our results. Parameters are not unique, but these are acceptable choices. We decided to make this spanning for two different models. The first one is the model which only takes in account the hydrolization reaction. The second one is the complete model, where we introduce the dimerization+oxidation process after hydrolization; for simplicity we do not consider backward reaction in the first process (of the second model), since parameters are copious. In both results we try to write the scale of intensity of the "turning on" as seen by experimental data, trying to give a range for every colour

Height (cm)	$\rho_p = 10^7$ cell/l		$\rho_p = 10^8$ cell/l		$\rho_p = 10^9$ cell/l	
	$t = 24\,h$	$t = 92\,h$	$t = 24\,h$	$t = 92\,h$	$t = 24\,h$	$t = 92\,h$
0,2						
0,4						
0,6						
0,8						
1,0						
1,2						
1,4						
1,6						
1,8						
2,0						

Height (cm)	$\rho_p = 10^7$ cell/l		$\rho_p = 10^8$ cell/l		$\rho_p = 10^9$ cell/l	
	$t = 24\,h$	$t = 92\,h$	$t = 24\,h$	$t = 92\,h$	$t = 24\,h$	$t = 92\,h$
0,2	0,003734	0,002345	0,02505	0,02093	0,06209	0,05648
0,4	0,164653	0,234510	0,647089	0,787281	0,977373	1,12437
0,6	0,377281	1,85603	1,29569	4,00917	1,86112	4,88499
0,8	0,503307	5,66296	1,61518	10,3861	2,27481	11,9599
1,0	0,569905	9,98070	1,77282	17,9407	2,47744	20,3052
1,2	0,603019	13,0126	1,84763	24,2525	2,57303	27,4409
1,4	0,618576	15,0346	1,88152	28,4446	2,61607	32,4192
1,6	0,625472	16,4550	1,89611	30,9579	2,63449	35,4673
1,8	0,628355	17,4505	1,90208	32,5830	2,64198	37,3616
2,0	0,629492	18,1411	1,90439	33,6767	2,64488	38,6154

OFF: $0 < [P] < 0,64\,nM$
SLIGHTLY ON: $0,64\,nM < [P] < 1,2\,nM$
ON: $1,2\,nM < [P] < 2\ nM$
STRONGLY ON: $[P] > 2\ nM$

Figure 4.8: Model 1: hydrolization process with backward reaction. Concentration in table is $[P]$ in nM in position $x = h$. Parameters: $\alpha = 7 \cdot 10^{-9} nMol/(cell \cdot h)$, $k = 0,05\ h^{-1}$, $A = 1\ nM/s$, $k_1 = 0,1\ h^{-1}$, $k_{-1} = 0,01\ h^{-1}$ $k_2 = 0,00001\ h^{-1}$.

In figure 4.8 we can see results of the first model for a suitable choice of parameters. Accordance with experimental data seems to be very good. Differences can be found just in the intensity of the "turning on".
In figure 4.9 we show results of the model which consider dimerization and oxidation. In this case results seem to be slightly less in accordance with experimental data in respect to the previous ones, but as always only in the intensity of the "turning on". Generally speaking, accordance is good in this situation, too. This

Height (cm)		$\rho_p = 10^7$ cell/l		$\rho_p = 10^8$ cell/l		$\rho_p = 10^9$ cell/l	
		$t = 24\,h$	$t = 92\,h$	$t = 24\,h$	$t = 92\,h$	$t = 24\,h$	$t = 92\,h$
0,2		0,000204	0,000178	0,006472	0,005651	0,03081	0,02691
0,4		0,15103	0,68980	2,45399	5,17020	5,5558	9,44815
0,6		0,60677	31,6755	7,11562	105,731	14,699	142,234
0,8		1,00608	187,110	10,2684	458,955	20,3128	558,123
1,0		1,24464	407,272	11,9460	950,821	23,2201	1124,62
1,2		1,36954	569,510	12,7428	1379,15	24,5781	1627,27
1,4		1,42649	685,349	13,0919	1666,15	25,1660	1981,75
1,6		1,45075	769,403	13,2347	1831,39	25,4043	2195,24
1,8		1,46037	828,480	13,2896	1939,21	25,4950	2321,71
2,0		1,46394	870,058	13,3095	2012,49	25,5275	2406,63

OFF: $0 < [L] < 2\,nM$

SLIGHTLY ON: $2\,nM < [L] < 10\,nM$

ON: $10\,nM < [L] < 14\,nM$

STRONGLY ON: $[L] > 14\,nM$

Figure 4.9: Model 2: hydrolization process without backward reaction, then dimerization+oxidation process. Concentration in table is $[L]$ in nM in position $x = h$. Parameters: $\alpha = 7 \cdot 10^{-9} nMol/(cell \cdot h)$, $k = 0,05\,h^{-1}$, $A = 1\,nM/s$, $k_1 = 1\,h^{-1}$, $k_2 = 0,001\,h^{-1}$ $k_p = 10\,h^{-1}$.

last study is much different and difficult than the previous one, since we introduce a point with special properties. In fact we assume that $x = h$ is the only point where dimerization+oxidation can take place. We are discussing this fact, because in the numerical process that we use to solve equations, we need to pay attention on the spatial discretization. If we do not use a sufficient fine spatial discretization, when we look at concentration in $x = h$, result could be affected by huge computational errors. This fact makes study very hard, because every single line must be adequatly discretized.

The main result which emerges from theoretical data, is that diffusion of X-Gal plays an important role in dynamics. We are not able to see the "turning on" of small lengths because diffusion permits X-Gal to escape before it can be attached by β-Gal. Moreover, it is important to notice that in both situations, k_2 is two order of magnitude smaller than k_1. This fact means that the first reaction is much faster than the second one. It seems to be a necessary condition and it is not sur-

prising, since it is in accordance with chemical properties of this kind of reactions [20]. However it is difficult to find precise chemical proves of the values of k_1, k_{-1}, k_2 and k_P, since our model is a huge semplification of all the complex underlying mechanism, therefore they are not the real chemical rates, but they include instead several hidden effects. Let's finally stress that among all parameters, the diffusion coefficient D of X-Gal is not a free parameter of the model, since we suppose it similar to that of AHL due to their similar size and chemical properties. In agar it was determined to be $D = 1,08\ mm^2/h$ [6].

A final particular can be added to our models. What we see from experimental data is not the real value of concentration, but only the colour which appears. It is then convenient to model final response with a sigmoidal function $\sigma(h, t)$. This means to introduce a function which takes final concentrations as values and gives back a number between 0 and 1. We can do that both for $[P]$ of the first model and $[L]$ of the second one. In both cases these functions are

$$\sigma_P(h, t) = \frac{1}{1 + \left(\frac{[P]^*}{[P](h,t)}\right)^{z_P}} \tag{4.5}$$

$$\sigma_L(h, t) = \frac{1}{1 + \left(\frac{[L]^*}{[L](h,t)}\right)^{z_L}} \tag{4.6}$$

Here, $[P]^*$ and $[L]^*$ are the concentration at which we decide the "turning on", they coincide with a concentration giving $\sigma(h, t) = 1/2$. We suppose that "turning on" is the darkest colour, so we set $[P]^* = 2\ nM$ and $[L]^* = 14\ nM$. Parameters z_P and z_L describe the slope of the function, it has the same role as m in figure 4.1. We set them to be $z_P = z_L = 1$. In practice, what we are introducing is a function of Hill's type. In Figure 4.10 we can see tables representing sigmoidal functions for the two models introduced above and their graphical representetion.

This concludes our study, which permitted us to find a complete and suitable model to describe experimental data. In this way we could describe size dependence as a mixed effect of signal dynamics, Quorum Sensing mechanism and subsequent X-Gal process with diffusion. This last ingredient is due to the indirect QS system that we decided to study. More direct QS mechanisms would probably let us to study system size dependence whern QS and signal molecules play a bigger role.

Height (cm)	$\rho_p = 10^7\ cell/l$		$\rho_p = 10^8\ cell/l$		$\rho_p = 10^9\ cell/l$	
	$t = 24\ h$	$t = 92\ h$	$t = 24\ h$	$t = 92\ h$	$t = 24\ h$	$t = 92\ h$
0,2	0,0019	0,0012	0,0124	0,0104	0,0301	0,0275
0,4	0,0761	0,1049	0,2445	0,2825	0,3283	0,3599
0,6	0,1587	0,4813	0,3931	0,6672	0,4820	0,7095
0,8	0,2011	0,7390	0,4468	0,8385	0,5321	0,8567
1,0	0,2218	0,8331	0,4699	0,8997	0,5533	0,9103
1,2	0,2317	0,8668	0,4802	0,9238	0,5627	0,9321
1,4	0,2362	0,8826	0,4847	0,9343	0,5667	0,9419
1,6	0,2382	0,8916	0,4867	0,9393	0,5685	0,9466
1,8	0,2391	0,8972	0,4875	0,9422	0,5691	0,9492
2,0	0,2394	0,9007	0,4878	0,9439	0,5694	0,9508

OFF: $0 < \sigma < 0,24$
SLIGHTLY ON: $0,24 < \sigma < 0,37$
ON: $0,37 < \sigma < 0,50$
STRONGLY ON: $\sigma > 0,50$
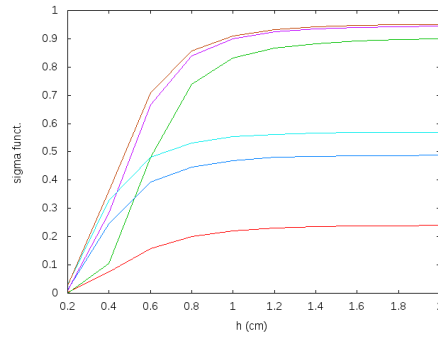
(a) σ_P

Height (cm)	$\rho_p = 10^7\ cell/l$		$\rho_p = 10^8\ cell/l$		$\rho_p = 10^9\ cell/l$	
	$t = 24\ h$	$t = 92\ h$	$t = 24\ h$	$t = 92\ h$	$t = 24\ h$	$t = 92\ h$
0,2	0,0001	0,0001	0,0004	0,0004	0,0022	0,0019
0,4	0,0107	0,0469	0,1491	0,2697	0,2841	0,4029
0,6	0,0415	0,6935	0,3370	0,8831	0,5122	0,9104
0,8	0,0670	0,9304	0,4231	0,9704	0,5920	0,9755
1,0	0,0816	0,9668	0,4604	0,9855	0,6239	0,9877
1,2	0,0891	0,9760	0,4765	0,9899	0,6371	0,9915
1,4	0,0924	0,9800	0,4832	0,9917	0,6425	0,9930
1,6	0,0938	0,9821	0,4860	0,9924	0,6447	0,9937
1,8	0,0944	0,9834	0,4870	0,9928	0,6455	0,9940
2,0	0,0946	0,9842	0,4874	0,9931	0,6458	0,9942

OFF: $0 < \sigma < 0,10$
SLIGHTLY ON: $0,10 < \sigma < 0,40$
ON: $0,40 < \sigma < 0,50$
STRONGLY ON: $\sigma > 0,50$

(b) σ_L
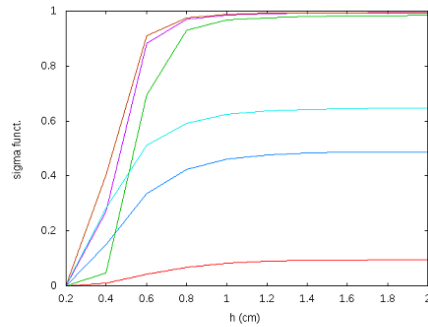
Figure 4.10: Sigmoidal functions for the two models discussed above. Different colours in the plot means different columns in the table. Plots should be points, but we link them with lines to make it more understandable.

Chapter 5

Conclusions and future outlooks

Bacterial Quorum Sensing is a cell-to-cell communication phenomenon that allows bacteria to control the expression of certain specialized genes. [5] Expression of these genes is controlled thorugh the concentration of particular signal molecules (AHL in the case of Gram negative bacteria). Once these molecules has reached a threshold level, these particular genes are transcribed and new expressions emerge. Bacteria population density has a big role in this mechanism, but simple physical models are able to show that also colony size could be significant. We first introduced two physical models which permit to think why system size dependence is reasonable, just looking at signal molecules dynamics (the key ingredient is their diffusion). Then we tried to prove it experimentally. The experiment that we set up consisted in cylinders of different heights with an absorbing boundary (baker with agar) and a reflecting one (air). Our aim was to model this system in order to understand the role of the system size.

Firstly, we modeled signal molecules dynamics in order to see if that was sufficient to explain experimental data. We divided space in three different environments: exterior, producers and reporters. We also considered the possiblity of molecules degradation. This dynamics was not sufficient to explain what we found in our experiment so we had to complete the model with the subsequent processes.

In fact, secondly, we made a model for the trigger of QS mechanism. This consisted in a link between signal molecules concentration and β-Gal enzyme production. We made it through a Hill's function.

Thirdly we had to describe the enzymatic reaction which takes place between β-Gal and X-Gal and the following dimerization of the product. A fundamental role was played by diffusion of small X-Gal molecules and their products. In fact this ingredient was the key to find a suitable description of experimental data.

Therefore, we can conclude that our experimental system is well described by a mix of three mechanisms. In particular a big role is given by the diffusion and the enzymatic reaction of X-Gal (and its products) which slightly hide the two pre-

vious processes. This is a consequence of the fact that the QS mechanism which was set up is very indirect. We are not able to directly see QS product (which is β-Gal) but we need to introduce a substrate to reveal it.

Two are the main ideas to improve this study.

The first is considering the same system but with a lower producers densitiy, because we hope that for lower densities our system turns on when cylinders are longer. So the diffusion at the reflecting boundary would have a marginal role (since we would be far from the absorbing boundary). Hence, we should repeat the experiment in order to obtain again our experimental data and to analyze the smaller density behaviour. This could confirm our model since signal molecules dynamics would be less hidden. This new experiment will be made soon by Andrea Squartini and his research group.
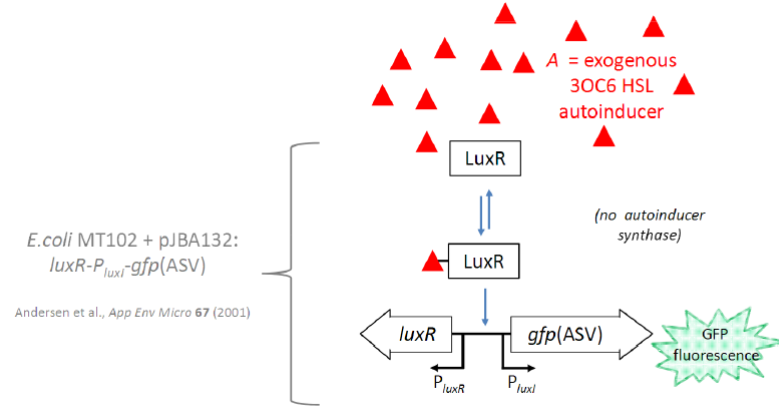

Figure 5.1: Quorum sensing system of a particular mutant of *Escherichia Coli*

The second idea is to completely change QS mechanism and to try a more direct QS system. This idea is given by [7]. It suggests us to build agar lanes where we put a particular mutant of *Escherichia coli* as they did (see Figure 5.1). Its Quorum Sensing expression is given by the production of the Green Fluorescent Protein (GFP) which is then revealed through a led excitation (see Figure 5.2). We want to modify their system in some aspects. They use exogenous AHL, while we want to have bacteria which produce AHL. Then, they use reflecting boundaries, while we want an absorbing boundary and a reflecting one. Therefore we want to build an analogous system of that we studied in this dissertation, but with a different system of producers/reporters. This could be a possible study, since we have the possibility to directly reveal the product of Quorum Sensing. Therefore we would avoid a huge dynamics after QS which could hide the threshold mecha-
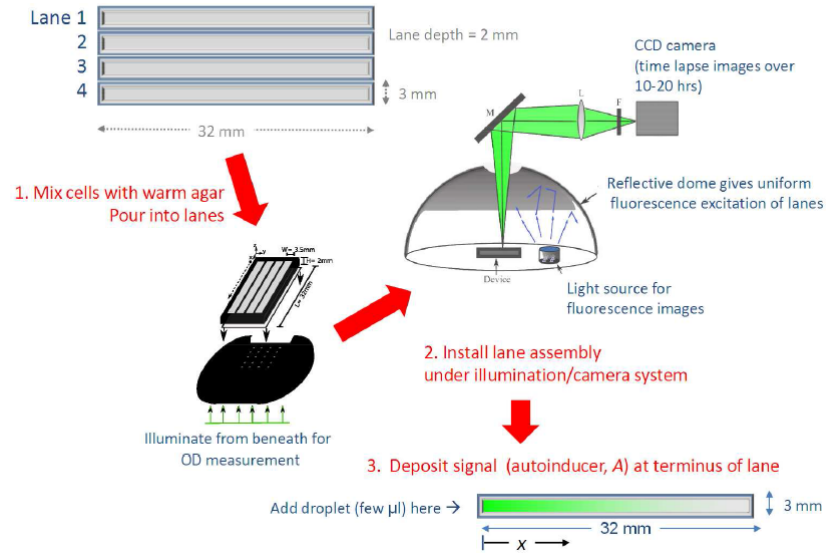
nism and signal dynamics.

Figure 5.2: Experimental set up of [7]

Results obtained through this dissertation are fundamental and with these two ideas we hope to improve our study in order to understand better system size dependence of QS. This could lead to a better control of Quorum Sensing mechanism for further biological and medical objectives.

Appendix A

Diffusion Equation: Analytical solution vs. Numerical solution

PROBLEM

An experiment is set up in order to have a one dimensional lane of length $h = 10\ mm$ filled with agarose and water. Both lane's boundaries in $x = 0$ and $x = h$ are supposed to be reflecting. At time $t = 0$ we put some dye in the first $\nu = 2\ mm$ of the lane. The dye diffuses through the lane and at $t = \infty$ it reaches a uniform distribution with concentration $C_\infty = 4\ nM$. Supposing the diffusion coefficient to be $D = 1,08\ mm^2/h$, calculate the analytical and the numerical solution of the diffusion equation $C(x,t)$ and compare the two results.

ANALYTICAL SOLUTION

We need to solve the equation

$$\frac{\partial C(x,t)}{\partial t} = D\frac{\partial^2 C(x,t)}{\partial x^2}$$

with initial conditions

$$C(x,0) = \begin{cases} C^* & if\ 0 \leq x \leq \nu \\ 0 & if\ \nu \leq x \leq h \end{cases}$$

where $C^* = \frac{C_\infty h}{\nu}$
and with boundary conditions

$$\frac{\partial C(x,t)}{\partial x}|_{x=0} = \frac{\partial C(x,t)}{\partial x}|_{x=h} = 0\ \forall\ t$$

The first step is to look for solutions of the diffusion equation of the type

$$C(x,t) = z(x)u(t)$$

79

If we substitute in the diffusion equation, we obtain

$$\frac{1}{u(t)}\frac{\partial u(t)}{\partial t} = \frac{D}{z(x)}\frac{\partial^2 z(x)}{\partial x^2}$$

The left side is indipendent from x, while the right side is indipendent from t, therefore they need to be independent both from x and t since they must to be equal. We can set them to be equal to a constant $A \neq 0$. In this way, we obtain a system of two equations:

$$\begin{cases} \frac{1}{u(t)}\frac{\partial u(t)}{\partial t} = A \\ \frac{D}{z(x)}\frac{\partial^2 z(x)}{\partial x^2} = A \end{cases}$$

These two differential equations are easily solvable, their solutions are:

$$\begin{cases} u(t) = u_0 e^{ADt} \\ z(x) = z_1 e^{\sqrt{A}x} + z_2 e^{-\sqrt{A}x} \end{cases}$$

Therefore we obtain the solution

$$C(x,t) = z(x)u(t) = (z_1 e^{\sqrt{A}x} + z_2 e^{-\sqrt{A}x})u_0 e^{ADt}$$

We need now to impose boundary conditions.

- $\frac{\partial C(x,t)}{\partial x}\big|_{x=0} = 0 \longrightarrow z_1 = z_2$

- $\frac{\partial C(x,t)}{\partial x}\big|_{x=h} = 0 \longrightarrow \sqrt{A} = in\frac{\pi}{h}$ where $n = 1, 2, ...$

These results lead to the family of solution depending on n

$$\begin{aligned} C_n(x,t) &= z_1 u_0 \left(e^{in\frac{\pi}{h}x} + e^{-in\frac{\pi}{h}x}\right) e^{-n^2\frac{\pi^2}{h^2}Dt} = \\ &= 2z_1 u_0 cos\left(n\frac{\pi}{h}x\right) e^{-n^2\frac{\pi^2}{h^2}Dt} = \\ &= a_0 cos(\omega_n x) e^{-\omega_n^2 Dt} \end{aligned}$$

where we set $a_0 = 2z_1 u_0$ and $\omega_n = n\pi/h$.
If $C_n(x,t)$ is one of the solution of this family, a generic solution of the diffusion equation is a linear combination of $C_n(x,t)$, where their coefficients a_n are not fixed. Therefore the general solution is

$$C(x,t) = \sum_{n=1}^{\infty} C_n(x,t) = \sum_{n=1}^{\infty} a_n cos(\omega_n x) e^{-\omega_n^2 Dt}$$

A very brief calculus shows that all C_n are orthogonal, in fact

$$\int_0^h \cos(\omega_n x)\cos(\omega_m x)dx = \frac{h}{2}\delta_{n,m}$$

We need now to determine a_n imposing the initial condition. Since

$$C(x,0) = \sum_{n=1}^{\infty} a_n \cos(\omega_n x)$$

using the orthogonality written above, we obtain

$$a_n = \frac{2}{h}\int_0^h C(x,0)\cos(\omega_n x)dx$$

Using now the initial condition of our problem, we get

$$a_n = \frac{2C_\infty}{\nu\omega_n}\sin(\omega_n\nu)$$

Therefore we obtain

$$C(x,t) = \frac{2C_\infty}{\nu}\sum_{n=1}^{\infty}\frac{\sin(\omega_n\nu)}{\omega_n}\cos(\omega_n x)e^{-\omega_n^2 Dt}$$

We need to impose a last condition: $C(x,\infty) = C_\infty$ since for a very long time concentration must be uniform with value C_∞. If we impose it, we obtain the final solution of the diffusion equation:

$$C(x,t) = C_\infty + \frac{2C_\infty}{\nu}\sum_{n=1}^{\infty}\frac{\sin(\omega_n\nu)}{\omega_n}\cos(\omega_n x)e^{-\omega_n^2 Dt} \tag{A.1}$$
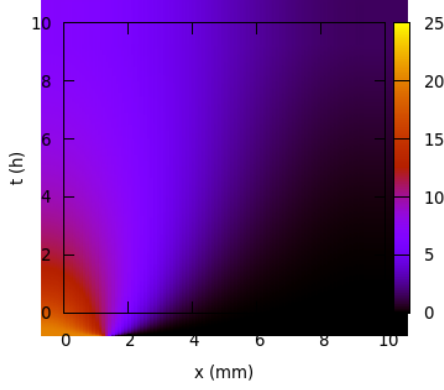
NUMERICAL SOLUTION
We want to write now a scheme which permits to calculate the solution of the diffusion equation in a numerical way. We decide to use the FTCS scheme. Hence we have the update formula
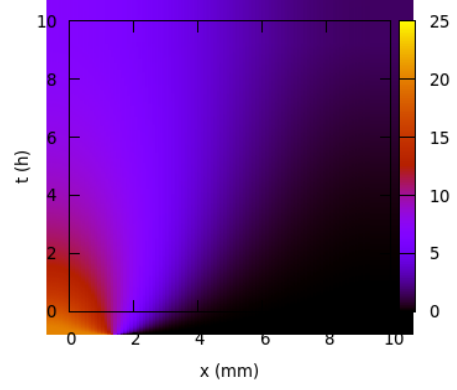
$$C_i^{j+1} = C_i^j + \frac{D\Delta t}{(\Delta x)^2}\left[C_{i+1}^j - 2C_i^j + C_{i-1}^j\right] \tag{A.2}$$

where i is the spatial index and P the number of spatial intervals:

$$i \in [0,P] \longrightarrow x = i\Delta x = \frac{ih}{P} \in [0,h]$$

(a) Analytical solution

(b) Numerical solution

and j is the temporal index and M the number of spatial intervals:

$$j \in [0, M] \longrightarrow t = j\Delta t = \frac{jt_{MAX}}{M} \in [0, t_{MAX}]$$

Initial conditions are

$$C_j^0 = \begin{cases} C^* & if \ 0 \leq i \leq i(\nu) \\ 0 & if \ i(\nu) \leq i \leq P \end{cases}$$

where $i(\nu)$ is the index of ν: $\nu = i(\nu)\Delta x$.
Boundary conditions are

$$\begin{cases} C_0^j = C_1^j & \forall j \in [0, M] \\ C_P^j = C_{P-1}^j & \forall j \in [0, M] \end{cases}$$

We need to be careful in the choice of M and P, since they need to satisfy the stability condition of the FTCS scheme:

$$\Delta t \leq \frac{1}{2}\frac{(\Delta x)^2}{D} \longrightarrow \alpha = \frac{D\Delta t}{(\Delta x)^2} \leq \frac{1}{2}$$

RESULTS COMPARISON
In Figure we show two plots of the dye's diffusion. They are three dimensional plots. On the x-axis we have space x (mm) while on the y-axis we have time t (h). Colour represents dye's concentration $C(x, t)$ (nM) and its scale can be seen near both plots. Lane's length is $h = 10 \ mm$ and $t_{MAX} = 10 \ h$.
Analytical solution (first figure) is calculated using the first $n = 50$ terms of the

series.

Numerical solution (second figure) is calculated with $M = 10000$ and $P = 100$. These values permit stability since $\alpha = 0,108 \leq 1/2$.

The two figures are almost the same. They both show how the dye slowly fills the entire lane, leading to a uniform distribution. Their similarity proves the power of the FTCS scheme. In fact this result encourages the use of the FTCS scheme to solve equations which need a numerical solution due to their complexity (as those we need to face).

Bibliography

[1] Melissa B. Miller and Bonnie L. Bassler. *Quorum Sensing in Bacteria*. Annu. Rev. Microbiol. 55:165-99 (2001).

[2] Costi D. Sifri. *Quorum Sensing: Bacteria Talk Sense*. Clinical Infectious Diseases 47:1070-6 (2008).

[3] Paul D. Shaw, Gao Ping, Sean L. Daly, Chung Cha, John E. Cronan, JR., Kenneth L. Rinehart, and Stephen K. Farrand. *Detecting and characterizing N-acyl-homoserine lactone signal molecules by thin-layer chromatography*. Proc. Natl. Acad. Sci. USA Vol.94, pp. 6036-6041 (2007).

[4] Simon Swift, John P. Throup, Paul Williams, George P. C. Salmonda and Gordon S. A. B. Stewart. *Quorum sensing: a population-density component in the determination of bacterial phenotype*. Tibs 21, 214-219 (1996).

[5] Anjali Kumari, Patrizia Pasini, Sapna K. Deo, Deborah Flomenhoft, Harohalli Shashidhar and Sylvia Daunert *Biosensing Systems for the Detection of Bacterial Quorum Signaling Molecules*. Anal. Chem. 78, 7603-7609 (2006)

[6] Antonio Trovato, Flavio Seno, Marina Zanardo, Sara Alberghini, Alessandra Tonello and Andrea Squartini *Quorum vs. diffusion sensing: a quantitative analysis of the relevance of absorbing or reflecting boundaries* FEMS Microbiol Lett 352, 198-203 (2014)

[7] Gabriel E. Dilanji, Jessica B. Langebrake, Patrick De Leenheer, and Stephen J. Hagen *Quorum Activation at a Distance: Spatiotemporal Patterns of Gene Regulation from Diffusion of an Autoinducer Signal* J. Am. Chem. Soc. 134, 5618-5626 (2012)

[8] Stephen C. Patt *Quorum sensing by encounter rates in the ant Temnothorax albipennis* Behav Ecol 16, 488-496 (2005)

[9] Andrea Squartini and Marina Zanardo *Personal communication* (2014)

[10] Englmann M, Fekete A, Kuttler C, Frommberg M, Li X, Gebefugi I, Fekete J and Schmitt-Kopplin P *The hydrolisis of unsibstituted N-acylhomoserine lactones to their homoserine metabolites. Analytical approaches using ultra performance liquid chromatography* J. Chromatogr A 1160, 184-193 (2007)

[11] Alberghini S, Polone E, Corich V, Carlot M, Seno F, Trovato A, Squartini A. *Consequences of relative cellulare positioning on quorum sensing and bacterial cell-to-cell communication* Fems Microbiology Letters, 242, 149-161 (2009)

[12] Johan H. J. Leveau and Steven E. Lindow *Predictive and Interpretive Simulation of Green Fluorescent Protein Expression in Reporter Bacteria* Journal of Bacteriology 183.20, 6752-6762 (2001)

[13] Christian Garde, Thomas Bjarnsholt, Michael Givskov, Tim Holm Jakobsen, Morten Hentzer, Anetta Claussen, Kim Sneppen, Jesper Ferkinghoff-Borg and Thomas Sams *Quorum Sensing Regulation in Aeromonas hydrophila* J. Mol. Biol. 396, 849-857 (2010)

[14] Otto Pulkkinen and Ralph Metzler *Distance Matters: The Impact of Gene Proximity in Bacterial Gene Regulation* Phys. Rev. Lett. 110, 198101 (2013)

[15] S. T. Rutherford and B. L. Bassler *Bacterial quorum sensing: its role in virulence and possibilities for its control* Cold Spring Harb. Perspect. Med. a012427 (2012)

[16] W. Claiborne Fuqua, Stephen C. Winans, and E. Peter Greenberg *Quorum Sensing in Bacteria: the LuxR-LuxI Family of Cell Density-Responsive Transcriptional Regulators* Journal of Bacteriology 176, 269-275 (1994)

[17] Johannes Muller, Christina Kuttler, Burkard A. Hense, Michael Rothballer, and Anton Hartmann *Cell-cell communication by quorum sensing and dimension reduction* J. Math Biol. 53, 672-702 (2006) and unpublished

[18] Nigel Goldenfeld and Leo P. Kadanoff *Simple Lessons from Complexity* Science 284, 87 (1999)

[19] Philip Nelson *Biological Physics: Energy, Information, Life.* (2003).

[20] Meyer B. Jackson *Molecular and Cellular Biophysics.* Cambridge University Press (2006).

[21] Victor P. Pikulin, Stanislav I. Pohozaev *Equations in Mathematical Physics: A pratical course.* Birkhauser (2001)

[22] William H. press, Saul A. teukolsky, William T. Vetterling, Brian P. Flannery *Numerical Recipes: The Art of Scientific Computing - Third Edition* Cambridge University Press (2007)

[23] John D. Andreson, Jr. *Computational Fluid Dynamics: the basic with application* McGraw-Hill (1995)

[24] Uri Alon *An Introduction to System Biology: Design Principles of Biological Circuits* Chapman & Hall/CRC Mathematical and Computational Biology Series (2007)

Ringraziamenti

Questo lavoro è il culmine di un lungo percorso iniziato cinque anni fa tra mille incertezze e dubbi ma che, anno dopo anno, si sono trasformati in passione. Passione verso una disciplina che spero possa portarmi tante soddisfazioni nella vita, a partire già dalla mia prossima meta, Trieste. Spero che quest'ultima possa essere solo l'inizio di un percorso attraverso il quale io possa trovare nuovi stimoli e obiettivi giorno dopo giorno.

La prima persona che voglio ringraziare è il mio relatore, il Prof. Seno, insieme al mio correlatore, il Dott. Trovato. Per la passione che hanno saputo trasmettermi verso la materia, per l'esperienza e la completa disponibilità dimostrata in questi mesi di lavoro e per avermi aiutato a mantenere la calma anche nei momenti più ardui.

Voglio ringraziare la mia famiglia, in particolare mia madre per avermi sempre dato supporto e consiglio, per aver sempre creduto in me e per avermi sempre dato la forza di affrontare la vita con grinta.

Voglio ringraziare i miei amici, perchè sono sempre riusciti a farmi sorridere anche nei momenti peggiori e perchè hanno sempre avuto la voglia di sopportarmi. I miei compagni di università, compagni di percorso, per le mille cene e risate fatte assieme.

Anche se abbiamo preso strade differenti, voglio ringraziare anche Anna, per avermi saputo ascoltare ed essere vicina in gran parte di questo lungo percorso. Ma soprattutto per avermi aiutato a crescere negli ultimi quattro anni e per avermi fatto conoscere quali sono i valori importanti della vita.

Dedico infine l'intero lavoro a mio padre che, anche se non ha potuto vedermi crescere, penso sarebbe sicuramente fiero del traguardo che ho raggiunto.

Padova, 30/09/2014

Mattia Marenda